

Charm-Meson t -channel Singularities in an Expanding Hadron Gas

Eric Braaten,^{1,*} Roberto Bruschini,^{1,†} Li-Ping He,^{2,‡} Kevin Ingles,^{1,§} and Jun Jiang^{3,¶}

¹*Department of Physics, The Ohio State University, Columbus, OH 43210, USA*

²*Helmholtz-Institut für Strahlen- und Kernphysik and Bethe Center for Theoretical Physics,
Universität Bonn, D-53115 Bonn, Germany*

³*School of Physics, Shandong University, Jinan, Shandong 250100, China*

(Dated: July 17, 2023)

Abstract

We study the time evolution of the numbers of charm mesons after the kinetic freezeout of the expanding hadron gas produced by the hadronization of the quark-gluon plasma from a central heavy-ion collision. The πD reaction rates have contributions from a D^* resonance in the s channel. The πD^* reaction rates are enhanced by t -channel singularities from an intermediate D . The contributions to reaction rates from D^* resonances and D -meson t -channel singularities are sensitive to thermal mass shifts and thermal widths. In the expanding hadron gas, the t -channel singularities are regularized by the thermal D widths. After kinetic freezeout, the thermal D widths are dominated by coherent pion forward scattering. The contributions to πD^* reaction rates from t -channel singularities are inversely proportional to the pion number density, which decreases to 0 as the hadron gas expands. The t -channel singularities produce small but significant changes in charm-meson ratios from those predicted using the known D^* -decay branching fractions.

Keywords: Charm mesons, effective field theory, heavy-ion collisions.

arXiv:2307.07470v1 [hep-ph] 14 Jul 2023

* braaten.1@osu.edu

† bruschini.1@osu.edu

‡ heliping@hiskp.uni-bonn.de

§ ingles.27@buckeyemail.osu.edu

¶ jiangjun87@sdu.edu.cn

I. INTRODUCTION

The charm mesons that are most easily observed in high-energy experiments are the pseudoscalar mesons D^+ and D^0 and the vector mesons D^{*+} and D^{*0} . The D 's have very long lifetimes because they decay by the weak interactions. The D^* 's are resonances whose widths are several orders of magnitude narrower than those of most hadron resonances. This remarkable feature arises because the D^*-D mass splittings are very close to the pion mass m_π , which limits the phase space available for those decays $D^* \rightarrow D\pi$ that are kinematically allowed. The soft pion in the rest frame of the D^* suppresses the rate for a hadronic decay $D^* \rightarrow D\pi$, making it comparable to that for a radiative decay $D^* \rightarrow D\gamma$.

Another consequence of D^*-D mass splittings being approximately equal to m_π is that there are charm-meson reactions with a t -channel singularity. A t -channel singularity is a divergence in the rate for a reaction in which an unstable particle decays and one of the particles from its decay is scattered [1]. The singularity arises because the scattered particle can be on shell. The adjective “ t -channel” refers to the fact that in the case of a $2 \rightarrow 2$ reaction, the scattered particle is exchanged in the t channel. The existence of t -channel singularities was first pointed out by Peierls in 1961 in the case of πN^* scattering through the exchange of a nucleon [2]. An example of a reaction with a t -channel singularity in the Standard Model of particle physics is $\nu_e Z^0 \rightarrow \nu_e Z^0$, which can proceed through the exchange of $\bar{\nu}_e$, which is one of the decay products in $Z^0 \rightarrow \nu_e \bar{\nu}_e$. The tree-level cross section diverges when the center-of-mass energy is greater than $\sqrt{2} M_Z$, because the $\bar{\nu}_e$ can be on shell. Another reaction with a t -channel singularity is $\mu^+ \mu^- \rightarrow W^+ e^- \bar{\nu}_e$, which can proceed through exchange of ν_μ , which is among the decay products in $\mu^- \rightarrow \nu_\mu e^- \bar{\nu}_e$. Melnikov and Serbo solved the divergence problem by taking into account the finite transverse sizes of the colliding μ^+ and μ^- beams [3].

A general discussion of t -channel singularities has been presented by Grzadkowski, Igllicki, and Mrówczyński [1]. They pointed out that if a reaction with a t -channel singularity occurs in a thermal medium, the divergence is regularized by the thermal width of the exchanged particle. The most divergent term in the reaction rate is replaced by a term inversely proportional to the thermal width. A general discussion of the thermal regularization of t -channel singularities has recently been presented by Igllicki [4].

The simplest charm-meson reactions with a t -channel singularity are $\pi D^* \rightarrow \pi D^*$. There are t -channel singularities in 6 of the 10 scattering channels: the elastic scattering of $\pi^0 D^{*+}$, $\pi^+ D^{*+}$, and $\pi^0 D^{*0}$ and the inelastic reactions $\pi^0 D^{*+} \rightarrow \pi^+ D^{*0}$, $\pi^+ D^{*0} \rightarrow \pi^0 D^{*+}$, and $\pi^- D^{*+} \rightarrow \pi^0 D^{*0}$. These reactions can proceed through the decay $D^* \rightarrow D\pi$ followed by the inverse decay $\pi D \rightarrow D^*$. The t -channel singularity arises because the intermediate D can be on shell. The cross section diverges when the center-of-mass energy squared, s , is in a narrow interval close to the threshold. In the case of the elastic scattering reaction $\pi D^* \rightarrow \pi D^*$, the t -channel singularity region is

$$2M_*^2 - M^2 + 2m_\pi^2 < s < (M_*^2 - m_\pi^2)^2/M^2, \quad (1)$$

where M_* and M are the masses of D^* and D . The lower endpoint of the interval is above the threshold $(M_* + m_\pi)^2$ by approximately $2M\delta$, where $\delta = M_* - M - m_\pi$. The small energy difference δ is comparable to isospin splittings. The difference between the upper and lower endpoints is approximately $8(M_*/M)m_\pi\delta$, which has a further suppression factor of m_π/M . The interval in the center-of-mass energy \sqrt{s} is largest for the reaction $\pi^0 D^{*0} \rightarrow \pi^0 D^{*0}$,

extending from 6.1 MeV to 8.1 MeV above the threshold $M_* + m_\pi = 2141.8$ MeV. Since the t -channel singularity arises because the intermediate D can be on-shell, the divergence in the cross section could be regularized by taking into account the tiny decay width Γ of the D , which would replace the divergent term by a term with a factor $1/\Gamma$. However, the resulting enormous cross section is unphysical. One reason is that the widths of the incoming and outgoing D^* are larger than Γ by about 8 orders of magnitude, so the D^* widths are more relevant than the width of D .

An obvious question is whether the t -channel singularities in charm-meson reactions have any observable consequences. One situation in which there may be observable consequences is the production of charm mesons in relativistic heavy-ion collisions. A central heavy-ion collision is believed to produce a hot dense region of quark-gluon plasma in which quarks and gluons are deconfined. The quark-gluon plasma expands and cools until it reaches the temperature for the crossover transition to a hadron resonance gas in which the quarks and gluons are confined into hadrons. After hadronization, the hadron resonance gas continues to expand and cool until it reaches kinetic freezeout, after which the momentum distributions of the hadrons are no longer affected by scattering. After kinetic freezeout, the hadron gas continues to expand as the hadrons free-stream away from the interaction region. The t -channel singularities in charm-meson reactions could have significant effects either during the expansion and cooling of the hadron resonance gas between hadronization and kinetic freezeout or during the expansion of the hadron gas after kinetic freezeout.

In the hadron gas produced by a heavy-ion collision, t -channel singularities are regularized by the thermal widths of the hadrons. The divergent term in the rate for a reaction with a t -channel singularity is replaced by a term inversely proportional to the thermal width of the hadron that can be on shell. Between hadronization and kinetic freezeout, the thermal widths are determined by the temperature. After kinetic freezeout, the thermal widths are determined by the temperature at kinetic freezeout and by the density of the system, which decreases as the hadron gas expands.

In this paper, we restrict our study of the effects of t -channel singularities in charm-meson reactions to the expanding hadron gas after kinetic freezeout. The restriction to after kinetic freezeout offers many simplifications. The only hadrons in the hadron resonance gas that remain are the most stable ones whose lifetimes τ are long enough that $c\tau$ is larger than the size of the hadron gas, whose order of magnitude is 10 fm. The most abundant hadrons by far are pions. The temperature at kinetic freezeout is low enough that the interactions of charm mesons and pions can be described by a chiral effective field theory. The relevant charm mesons are D^+ , D^0 , D^{*+} , and D^{*0} . The decays of D^{*+} and D^{*0} , whose lifetimes satisfy $c\tau > 2000$ fm, occur long after kinetic freezeout. The dominant contribution to the thermal width of a charm meson comes from the coherent forward scattering of pions and is proportional to the pion number density \mathbf{n}_π , which decreases to 0 as the hadron gas expands. A D -meson t -channel singularity therefore gives a contribution to the reaction rate inversely proportional to \mathbf{n}_π . The factor of $1/\mathbf{n}_\pi$ can cancel a multiplicative factor of \mathbf{n}_π in a term in a rate equation, increasing the importance of that term at late times. In Ref. [5], we showed that D -meson t -channel singularities in the reactions $\pi D^* \rightarrow \pi D^*$ produce significant modifications to the ratios of charm mesons produced by heavy-ion collisions. In this paper, we present the details of the calculations that lead to this surprising result.

The rest of the paper is organized as follows. In Section II, we establish our notation for various properties of charm mesons. In Section III, we describe the hadron resonance

gas produced by a heavy-ion collision and we present a simple model for its time evolution. In Section IV, we calculate the mass shifts and thermal widths of charm meson in a pion gas. In Section V, we calculate reaction rates of charm meson and pions in a pion gas. In Section VI, we solve the rate equations for the charm-meson number densities in the expanding hadron gas produced by a heavy-ion collision after kinetic freezeout. We show that D -meson t -channel singularities produce small but significant changes in the ratios of charm-meson abundances. We summarize our results in Section VII. In Appendix A, we give the Feynman rules for heavy-hadron χ EFT used in the calculations in Sections IV and V. In Appendix B, we calculate a thermal average over the pion momentum distribution that is sensitive to isospin splittings.

II. CHARM MESONS

In this section, we introduce notation for the masses and decay widths of charm mesons. We also describe simple relations between numbers of charm mesons that involve D^* branching fractions.

A. Masses and widths

We denote the masses of the pseudoscalar charm mesons D^+ and D^0 by M_+ and M_0 and the masses of the vector charm mesons D^{*+} and D^{*0} by M_{*+} and M_{*0} . We denote the $D^{*a} - D^b$ mass difference by $\Delta_{ab} = M_{*a} - M_b$. The average of the four mass differences is $\Delta = 141.3$ MeV. We denote the masses of the pions π^\pm and π^0 by m_{π^\pm} and m_{π^0} . We sometimes also denote the mass of the pion produced in the transition $D^{*a} \rightarrow D^b\pi$ by $m_{\pi ab}$: $m_{\pi ab} = m_{\pi^0}$ if $a = b$, $m_{\pi ab} = m_{\pi^\pm}$ if $a \neq b$. When isospin splittings can be neglected, we take the pion mass m_π to be the average over the three pion flavors: $m_\pi = 138.0$ MeV. Many reaction rates are sensitive to the difference between a D^* mass and a $D\pi$ scattering threshold. The differences for the transitions $D^* \rightarrow D\pi$ that conserve electric charge are

$$\Delta_{00} - m_{\pi^0} = 7.04 \pm 0.03 \text{ MeV}, \quad (2a)$$

$$\Delta_{+0} - m_{\pi^+} = 5.855 \pm 0.002 \text{ MeV}, \quad (2b)$$

$$\Delta_{++} - m_{\pi^0} = 5.63 \pm 0.02 \text{ MeV}, \quad (2c)$$

$$\Delta_{0+} - m_{\pi^+} = -2.38 \pm 0.03 \text{ MeV}. \quad (2d)$$

The negative value of $\Delta_{0+} - m_{\pi^+}$ implies that the decay $D^{*0} \rightarrow D^+\pi^-$ is kinematically forbidden.

We denote the total decay widths of the vector charm mesons D^{*+} and D^{*0} by Γ_{*+} and Γ_{*0} . The decay width of D^{*+} is measured. The decay width of D^{*0} can be predicted using Lorentz invariance, chiral symmetry, isospin symmetry, and measured D^* branching fractions:

$$\frac{\text{Br}[D^{*0} \rightarrow D^0\pi^0] \Gamma_{*0}}{\text{Br}[D^{*+} \rightarrow D^0\pi^+] \Gamma_{*+}} = \frac{\lambda^{3/2}(M_{*0}^2, M_0^2, m_{\pi^0}^2)/M_{*0}^5}{2\lambda^{3/2}(M_{*+}^2, M_0^2, m_{\pi^+}^2)/M_{*+}^5}, \quad (3)$$

where $\lambda(x, y, z) = x^2 + y^2 + z^2 - 2(xy + yz + zx)$. The branching fractions for the decays $D^* \rightarrow D\pi$ are

$$B_{+0} \equiv \text{Br}[D^{*+} \rightarrow D^0\pi^+] = (67.7 \pm 0.5)\%, \quad (4a)$$

$$B_{00} \equiv \text{Br}[D^{*0} \rightarrow D^0\pi^0] = (64.7 \pm 0.9)\%, \quad (4b)$$

$$B_{++} \equiv \text{Br}[D^{*+} \rightarrow D^+\pi^0] = (30.7 \pm 0.5)\%. \quad (4c)$$

The D^* decay widths are

$$\Gamma_{*+} \equiv \Gamma[D^{*+}] = 83.4 \pm 1.8 \text{ keV}, \quad (5a)$$

$$\Gamma_{*0} \equiv \Gamma[D^{*0}] = 55.4 \pm 1.5 \text{ keV}. \quad (5b)$$

The D^* radiative decay rates are

$$\Gamma_{*+, \gamma} \equiv \Gamma[D^{*+} \rightarrow D^+\gamma] = 1.3 \pm 0.3 \text{ keV}, \quad (6a)$$

$$\Gamma_{*0, \gamma} \equiv \Gamma[D^{*0} \rightarrow D^0\gamma] = 19.6 \pm 0.7 \text{ keV}. \quad (6b)$$

The decay widths of the spin-0 charm mesons D^+ and D^0 are smaller than those for D^* by about 8 orders of magnitude, because they only decay through weak interactions.

The interactions of low-energy pions with momenta at most comparable to m_π can be described by chiral effective field theory (χ EFT) [6]. The self-interactions of pions in χ EFT at leading order (LO) are determined by the pion decay constant f_π . It can be determined from the partial decay rate for π^+ into $\mu^+\nu_\mu$:

$$\Gamma[\pi^+ \rightarrow \mu^+\nu_\mu] = \frac{1}{8\pi} |V_{ud}|^2 G_F^2 f_\pi^2 \frac{m_\mu^2 (m_{\pi^+}^2 - m_\mu^2)^2}{m_{\pi^+}^3}. \quad (7)$$

From the measured decay rate, we obtain $f_\pi = 131.7 \text{ MeV}$.

The interactions of charm mesons with low-energy pions can be described by heavy-hadron χ EFT (HH χ EFT) [7–9]. The first-order corrections in HH χ EFT include terms suppressed by m_π/M and Δ/M . Isospin splittings can be treated as second-order corrections. The partial decay rate for $D^* \rightarrow D\pi$ in HH χ EFT at LO is sensitive to isospin splittings through a multiplicative factor $(\Delta^2 - m_\pi^2)^{3/2}$. Isospin splittings can be taken into account in the partial decay rate for $D^{*a} \rightarrow D^b\pi$ by replacing Δ by $\Delta_{ab} = M_{*a} - M_b$ and m_π by the mass $m_{\pi ab}$ of the emitted pion. The resulting expression for the partial decay rate is

$$\Gamma[D^{*a} \rightarrow D^b\pi] = \frac{g_\pi^2}{12\pi f_\pi^2} (2 - \delta_{ab}) (\Delta_{ab}^2 - m_{\pi ab}^2)^{3/2} \theta(\Delta_{ab} - m_{\pi ab}). \quad (8)$$

The dimensionless coupling constant g_π can be determined from measurements of the decay $D^{*+} \rightarrow D^0\pi^+$: $g_\pi = 0.520 \pm 0.006$.

B. Charm-meson numbers

The numbers of charm hadrons created in a high-energy collision must be inferred from the numbers that are detected. The decay of D^{*0} always produces D^0 . The decay of D^{*+} produces D^0 and D^+ with branching fractions B_{+0} and $1 - B_{+0}$. We denote the numbers of

D^0 , D^+ , D^{*0} , and D^{*+} observed in some kinematic region by N_{D^0} , N_{D^+} , $N_{D^{*0}}$, and $N_{D^{*+}}$. The observed numbers of D^0 and D^+ can be predicted in terms of the numbers $(N_{D^a})_0$ and $(N_{D^{*a}})_0$ before D^* decays and the branching fraction B_{+0} :

$$N_{D^0} = (N_{D^0})_0 + (N_{D^{*0}})_0 + B_{+0} (N_{D^{*+}})_0, \quad (9a)$$

$$N_{D^+} = (N_{D^+})_0 + 0 + (1 - B_{+0}) (N_{D^{*+}})_0. \quad (9b)$$

The last two terms in each equation come from D^{*0} and D^{*+} decays, respectively. The difference between the numbers of D^0 and D^+ can be expressed as

$$N_{D^0} - N_{D^+} = 2B_{+0} (N_{D^{*+}})_0 + (N_{D^0} - N_{D^+})_0 + (N_{D^{*0}} - N_{D^{*+}})_0. \quad (10)$$

The simple relations in Eqs. (9) have been assumed in all previous analyses of charm-meson production. We will show in this paper that these relations can be modified by t -channel singularities.

In a high-energy hadron collision, the numbers of D^0 and D^+ created in some kinematic region should be approximately equal by isospin symmetry: $(N_{D^0})_0 \approx (N_{D^+})_0$. Similarly, the numbers of D^{*0} and D^{*+} created should be approximately equal: $(N_{D^{*0}})_0 \approx (N_{D^{*+}})_0$. The deviations from isospin symmetry in the charm cross section should be negligible, because isospin splittings are tiny compared to the energy available for producing additional hadrons. The decays of bottom hadrons give isospin-violating contributions to charm-meson production, but the bottom cross section is much smaller than the charm cross section at present-day colliders.

The charm mesons that are most easily observed at a hadron collider are D^0 , D^+ , and D^{*+} , because they have significant decay modes with all charged particles. If the only reactions of charm mesons after their production are D^* decays, the ratios of the observed numbers of D^0 , D^+ , and D^{*+} are determined by the vector/pseudoscalar ratio before D^* decays, which we denote by $(N_{D^*}/N_D)_0$. Assuming isospin symmetry, that ratio can be expressed in terms of the observed numbers N_{D^0} , N_{D^+} , and $N_{D^{*+}}$:

$$\left(\frac{N_{D^*}}{N_D}\right)_0 \approx \frac{2N_{D^{*+}}}{N_{D^0} + N_{D^+} - 2N_{D^{*+}}}. \quad (11)$$

Isospin symmetry also implies that there is a combination of the three observed numbers that is completely determined by B_{+0} :

$$\frac{N_{D^0} - N_{D^+}}{N_{D^{*+}}} \approx 2B_{+0} = 1.35 \pm 0.01. \quad (12)$$

Deviations from this prediction must come either from initial conditions that deviate from isospin symmetry or from charm-meson reactions other than D^* decays that also violate isospin symmetry. Reactions with t -channel singularities are examples of such reactions.

III. HEAVY-ION COLLISIONS

In this section, we present a simple model for the hadron resonance gas produced by a central relativistic heavy-ion collision. We describe the Statistical Hadronization Model for the abundances of hadrons produced by a heavy-ion collision. Finally we describe the number densities of pions and charm mesons both before and after the kinetic freezeout of the hadron gas.

A. Expanding hadron gas

The central collision of relativistic heavy ions is believed to produce a quark-gluon plasma (QGP) consisting of deconfined quarks and gluons which then evolves into a hadron resonance gas (HRG) consisting of hadrons. A heavy-ion collision involves multiple stages: the collisions of the Lorentz-contracted nucleons in the nuclei, the formation and thermalization of the QGP, the expansion and cooling of the QGP, the hadronization of the QGP into the HRG, the expansion and cooling of the HRG as most of the resonances decay, the kinetic freezeout of the HRG when its density becomes too low for collisions to change momentum distributions, and finally the expansion of the resulting hadron gas by the free-streaming of hadrons. For each stage, complicated phenomenological models have been developed to provide quantitative descriptions [10–14].

A natural variable to describe the space-time evolution of the system created by the heavy-ion collision is the proper time τ since the collision. A simple phenomenological model that may describe the essential features of the system between the equilibration of the QGP and the kinetic freezeout of the HRG is a homogeneous system with volume $V(\tau)$ in thermal equilibrium at temperature $T(\tau)$. We denote the proper time just after hadronization by τ_H and the proper time at kinetic freezeout by τ_{kf} . The volume increases from V_H at τ_H to V_{kf} at τ_{kf} , while the temperature decreases from T_H to T_{kf} . These proper times, volumes, and temperatures can be determined by fitting the outputs of simplified hydrodynamic models for heavy-ion collisions. Values of the volumes V_H and V_{kf} and the temperatures T_H and T_{kf} for various heavy-ion colliders are given in Refs. [15, 16]. An explicit parametrization of the volume $V(\tau)$ can be obtained by assuming the boost-invariant longitudinal expansion proposed by Bjorken [17] and an accelerated transverse expansion caused by the pressure of the QGP before hadronization and by the pressure of the HRG after hadronization [18]. The parametrization of $V(\tau)$ for the HRG between hadronization and kinetic freezeout is [19]

$$V(\tau) = \pi [R_H + v_H(\tau - \tau_H) + a_H(\tau - \tau_H)^2/2]^2 c\tau \quad (\tau_H < \tau < \tau_{\text{kf}}), \quad (13)$$

where R_H , v_H , and a_H are the transverse radius, velocity, and acceleration at τ_H . If the transverse velocity $v_H + a_H(\tau - \tau_H)$ reaches the speed of light before kinetic freezeout, the subsequent transverse expansion proceeds at the constant velocity c . The temperature $T(\tau)$ can be determined by assuming isentropic expansion. The parametrization of $T(\tau)$ for the HRG between hadronization and kinetic freezeout in Ref. [20] is

$$T(\tau) = T_H + (T_{\text{kf}} - T_H) \left(\frac{\tau - \tau_H}{\tau_{\text{kf}} - \tau_H} \right)^{4/5} \quad (\tau_H < \tau < \tau_{\text{kf}}). \quad (14)$$

The parameters in $V(\tau)$ and $T(\tau)$ for central Pb-Pb collisions at 5.02 TeV are given in Ref. [21]. Hadronization and kinetic freezeout occur at the proper times $\tau_H = 10.2$ fm/ c and $\tau_{\text{kf}} = 21.5$ fm/ c . Between hadronization and kinetic freezeout, the temperature decreases from $T_H = 156$ MeV to $T_{\text{kf}} = 115$ MeV. The transverse radius increases from $R_H = 13.0$ fm to 24.0 fm. The transverse speed increases from $v_H = 0.78c$ to c at $\tau = 12.7$ fm/ c and then remains constant at $v_{\text{kf}} = c$.

After kinetic freezeout, the system continues to expand, but the momentum distributions of the hadrons are those for a fixed temperature: $T(\tau) = T_{\text{kf}}$. A simple model for the volume $V(\tau)$ is continued longitudinal expansion at the speed of light and transverse expansion at

the same speed v_{kf} as at kinetic freezeout:

$$V(\tau) = \pi [R_{\text{kf}} + v_{\text{kf}}(\tau - \tau_{\text{kf}})]^2 c\tau \quad (\tau > \tau_{\text{kf}}). \quad (15)$$

We assume the system remains homogeneous throughout the expanding volume $V(\tau)$. In the absence of further interactions, the number density for each stable hadron would decrease in proportion to $1/V(\tau)$ as τ increases.

Charm quarks and antiquarks are created in the hard collisions of the nucleons that make up the heavy ions. Charm quarks are assumed to quickly thermalize with the QGP at the temperature $T(\tau)$. They are not in chemical equilibrium, because the temperature of the QGP is too low for gluon and light-quark collisions to create charm quark-antiquark pairs. The low density of charm quarks suppresses the annihilation of charm quarks and antiquarks, so the charm-quark and charm-antiquark numbers are essentially conserved. Conservation of charm-quark number determines the charm-quark fugacity $g_c(\tau)$ in terms of the temperature $T(\tau)$ and the volume $V(\tau)$. After hadronization, charm hadrons are in thermal equilibrium with the HRG at the temperature $T(\tau)$. Their number densities evolve according to rate equations consistent with the conservation of charm-quark number. The charm hadrons are assumed to remain in thermal equilibrium until kinetic freezeout, after which they free-stream to the detector.

B. Statistical Hadronization Model

The Statistical Hadronization Model (SHM) is a model for the abundances of hadrons produced by a heavy-ion collision [22]. According to the SHM, the hadronization of the QGP into the HRG occurs while they are in chemical and thermal equilibrium with each other at a specific hadronization temperature T_H that can be identified with the temperature of the crossover between the QGP and the HRG. At hadronization, the number density of any spin state of a light hadron depends only on the hadron mass and the temperature T_H . (At sufficiently high rapidity or at lower heavy-ion collision energies, a number density can also depend on the baryon chemical potential.) The SHM takes into account the subsequent decays of hadron resonances, which increase the abundances of the lighter and more stable hadrons. The SHM does not take into account the scattering reactions that allow the HRG to remain in thermal equilibrium after hadronization.

The SHM can also describe the abundances of charm hadrons produced by a heavy-ion collision [23]. According to the SHM, charm hadrons are created during hadronization while the QGP and HRG are in thermal equilibrium at the temperature T_H . At hadronization, the number density of any spin state of a charm hadron is determined only by its mass, the hadronization temperature T_H , and multiplicative factors of the charm-quark fugacity g_c . The number density of a charm hadron with a single charm quark or antiquark is larger than the number density in chemical equilibrium by the factor g_c . The number density of a hadron whose heavy constituents consist of n charm quarks and antiquarks is larger than the number density in chemical equilibrium by g_c^n [24].

The SHM gives simple predictions for charm-hadron ratios at hadronization. Since the mass of a charm hadron is so large compared to $T(\tau)$, its momentum distribution in the HRG can be approximated by a relativistic Boltzmann distribution. The charm-hadron fugacity enters simply as a multiplicative factor. At hadronization, the charm-hadron fugacity is the

product of the charm-quark fugacity g_c and the number of spin states. The factor of g_c cancels in ratios of charm-hadron number densities. The ratio of the numbers of vector and pseudoscalar charm mesons at hadronization is predicted to be

$$\frac{N_{D^*}}{N_D} = 3 \frac{M_*^2 K_2(M_*/T_H)}{M^2 K_2(M/T_H)}, \quad (16)$$

where M and M_* are the masses of D and D^* , which we take to be the isospin averages of the masses of the pseudoscalar and vector charm mesons, respectively. At the hadronization temperature $T_H = 156$ MeV, the vector/pseudoscalar ratio is predicted to be $N_{D^*}/N_D = 1.339$. Ratios of the charm-hadron number densities for isospin partners are given by equations analogous to Eq. (16) but without the factor of 3. The predicted ratio for pseudoscalar charm mesons at hadronization is $N_{D^0}/N_{D^+} = 1.028$. The predicted ratio for vector charm mesons at hadronization is $N_{D^{*0}}/N_{D^{*+}} = 1.020$. The SHM predictions for charm-hadron ratios are modified from the simple predictions at hadronization by the feeddown from the decays of higher charm-hadron resonances.

The SHM has been applied to Pb-Pb collisions for at nucleon-nucleon center-of-mass energy $\sqrt{s_{NN}} = 5.02$ TeV in Ref. [24] for various centrality bins; we choose to focus only on the most central collisions. The charm-quark fugacity at hadronization has been determined to be $g_c = 29.6 \pm 5.2$. Predictions for the multiplicities dN/dy for 4 charm mesons and 2 charm baryons at midrapidity ($|y| < \frac{1}{2}$) are given in Table 1 of Ref. [24]. The expanding hadron gas is modeled by a “core” in which the formation of charm hadrons is described by the SHM and a “corona” in which their formation is described by that in pp collisions. For collisions in the centrality range 0-10%, the predicted multiplicities dN/dy from the core for D^0 , D^+ , and D^{*+} are 6.02, 2.67, and 2.36, respectively, with error bars consistent with those from a multiplicative factor of $g_c = 29.6 \pm 5.2$. The error bars on ratios of the multiplicities should be much smaller than 18%, but they cannot be determined from the results presented in Ref. [24]. The predicted additional multiplicities dN/dy from the corona for D^0 , D^+ , and D^{*+} are 0.396, 0.175, and 0.160, respectively. The effect of the corona is to increase all three multiplicities by about 7%.

An SHM prediction for the vector/pseudoscalar ratio before D^* decays can be obtained by inserting the predicted total multiplicities for D^0 , D^+ , and D^{*+} into Eq. (11): $(N_{D^*}/N_D)_0 = 1.194$. This is significantly smaller than the ratio 1.339 at hadronization predicted by Eq. (16), but also includes feeddown effects from decays of higher resonances. The SHM prediction for the ratio $(N_{D^0} - N_{D^+})/N_{D^{*+}}$ is 1.42. This is larger than the isospin-symmetry prediction 1.35 in Eq. (12) by about 5%. This, in turn, is larger than the thermal isospin-symmetry deviations at hadronization predicted by the SHM, which are less than 3%.

C. Pion momentum distributions

The temperature T of the HRG is comparable to the pion mass m_π . By isospin symmetry, the pions π^- , π^0 , and π^+ all have the same number density \mathbf{n}_π . The number density for pions in chemical and thermal equilibrium at temperature T is

$$\mathbf{n}_\pi^{(\text{eq})} = \int \frac{d^3q}{(2\pi)^3} \frac{1}{e^{\beta\omega_q} - 1}, \quad (17)$$

where $\omega_q = \sqrt{m_\pi^2 + q^2}$ and $\beta = 1/T$ is the inverse temperature. At the kinetic freezeout temperature $T_{\text{kf}} = 115$ MeV, the equilibrium number density is $\mathbf{n}_\pi^{(\text{kf})} = 1/(3.95 \text{ fm})^3$.

Between hadronization and kinetic freezeout, the pions are in chemical and thermal equilibrium. The temperature $T(\tau)$ of the HRG decreases as the proper time τ increases. The momentum distribution \mathbf{f}_π of the pions is the Bose-Einstein distribution:

$$\mathbf{f}_\pi(\omega_q) = \frac{1}{e^{\beta\omega_q} - 1} \quad (\tau_H < \tau < \tau_{\text{kf}}), \quad (18)$$

where $\beta = 1/T(\tau)$. The temperature $T(\tau)$ can be parametrized as in Eq. (14).

After kinetic freezeout, the temperature remains constant: $T(\tau > \tau_{\text{kf}}) = T_{\text{kf}}$. The pion number density decreases in inverse proportion to the volume $V(\tau)$ of the expanding hadron gas:

$$\mathbf{n}_\pi(\tau) = \frac{V_{\text{kf}}}{V(\tau)} \mathbf{n}_\pi^{(\text{kf})} \quad (\tau > \tau_{\text{kf}}), \quad (19)$$

where $\mathbf{n}_\pi^{(\text{kf})}$ is the equilibrium pion number density in Eq. (17) at the temperature T_{kf} and V_{kf} is the volume of the hadron gas at kinetic freezeout. The volume $V(\tau)$ can be parametrized as in Eq. (15). The normalization of the momentum distribution \mathbf{f}_π of the pions is determined by the pion number density \mathbf{n}_π :

$$\mathbf{f}_\pi(\omega_q) = \frac{\mathbf{n}_\pi}{\mathbf{n}_\pi^{(\text{kf})}} \frac{1}{e^{\beta_{\text{kf}}\omega_q} - 1} \quad (\tau > \tau_{\text{kf}}), \quad (20)$$

where $\beta_{\text{kf}} = 1/T_{\text{kf}}$.

We use angular brackets to denote the average over the momentum distribution of a pion. The thermal average of a function $F(\mathbf{q})$ of the pion momentum is

$$\langle F(\mathbf{q}) \rangle = \int \frac{d^3q}{(2\pi)^3} \mathbf{f}_\pi(\omega_q) F(\mathbf{q}) \Big/ \int \frac{d^3q}{(2\pi)^3} \mathbf{f}_\pi(\omega_q). \quad (21)$$

The thermal average depends on the temperature T . After kinetic freezeout, the pion number density \mathbf{n}_π cancels in the thermal average in Eq. (21). If the thermal average is sensitive to the flavor i of the pion, the pion energy in Eq. (21) should be replaced by $\omega_{iq} = \sqrt{m_{\pi_i}^2 + q^2}$.

The multiplicities of π^+ and π^- produced by Pb-Pb collisions at the LHC with $\sqrt{s_{NN}} = 5.02$ TeV have been measured by the ALICE collaboration [25]. The pion multiplicity averaged over π^+ and π^- from collisions in the centrality range 0-10% is

$$dN_\pi/dy = 769 \pm 34. \quad (22)$$

The total pion multiplicity for π^+ , π^- , and π^0 is 3 times larger. A fit of the SHM to hadron abundances at midrapidity in Pb-Pb collisions at the LHC with $\sqrt{s_{NN}} = 2.76$ TeV has been presented in Ref. [26]. The central values of the SHM fits for the multiplicities of π^+ and π^- are lower than the data by about 10% , which is comparable to the experimental error bars.

D. Charm-meson momentum distributions

We denote the number densities of the charm mesons D^+ , D^0 , D^{*+} , and D^{*0} in the hadron gas by \mathbf{n}_{D^+} , \mathbf{n}_{D^0} , $\mathbf{n}_{D^{*+}}$, and $\mathbf{n}_{D^{*0}}$, respectively. Since charm-meson masses are so much larger than the temperature T , the momentum distributions of the charm mesons can be approximated by relativistic Boltzmann distributions. If the charm mesons were in both chemical and thermal equilibrium, their number densities would be determined by the temperature T :

$$\mathbf{n}_{D^a}^{(\text{eq})} = \int \frac{d^3q}{(2\pi)^3} \exp(-\beta\sqrt{M_a^2 + p^2}) = \frac{M_a^2 K_2(M_a/T)}{2\pi^2/T}, \quad (23a)$$

$$\mathbf{n}_{D^{*a}}^{(\text{eq})} = 3 \int \frac{d^3q}{(2\pi)^3} \exp(-\beta\sqrt{M_{*a}^2 + p^2}) = \frac{3 M_{*a}^2 K_2(M_{*a}/T)}{2\pi^2/T}. \quad (23b)$$

However the charm mesons in the expanding hadron gas are not in chemical equilibrium. The number densities $\mathbf{n}_{D^a}(\tau)$ and $\mathbf{n}_{D^{*a}}(\tau)$ evolve with the proper time according to rate equations consistent with the conservation of charm-quark number. The momentum distributions of the charm mesons are

$$\mathbf{f}_{D^a}(\mathbf{p}) = \frac{\mathbf{n}_{D^a}}{\mathbf{n}_{D^a}^{(\text{eq})}} \exp(-\beta\sqrt{M_a^2 + p^2}), \quad (24a)$$

$$\mathbf{f}_{D^{*a}}(\mathbf{p}) = 3 \frac{\mathbf{n}_{D^{*a}}}{\mathbf{n}_{D^{*a}}^{(\text{eq})}} \exp(-\beta\sqrt{M_{*a}^2 + p^2}). \quad (24b)$$

Before kinetic freezeout, the number densities $\mathbf{n}_{D^a}(\tau)$ and $\mathbf{n}_{D^{*a}}(\tau)$ evolve according to rate equations that take into account charm-meson reactions and the expanding volume $V(\tau)$. After kinetic freezeout, the temperature remains constant at T_{kf} , so $\beta = \beta_{\text{kf}}$. In the absence of further interactions, $\mathbf{n}_{D^a}(\tau)$ and $\mathbf{n}_{D^{*a}}(\tau)$ would decrease in proportion to $1/V(\tau)$ as τ increases, just like the pion number density in Eq. (19). At very large proper times ($c\tau > 2,000$ fm), the D^* 's decay into D 's.

The multiplicities of charm hadrons in central Pb-Pb collisions at $\sqrt{s_{NN}} = 5.02$ TeV have been predicted using SHM in Ref. [24]. For collisions in the centrality range 0-10%, the central values of the predicted multiplicities dN/dy at midrapidity for D^0 , D^+ , and D^{*+} are 6.42, 2.84, and 2.52. No prediction was given for the multiplicity of D^{*0} . We can estimate the multiplicity of D^{*0} by assuming that the ratio of the numbers of D^{*0} and D^{*+} is the same as at hadronization:

$$\frac{N_{*0}}{N_{*+}} = \frac{M_{*0}^2 K_2(M_{*0}/T_H)}{M_{*+}^2 K_2(M_{*+}/T_H)}. \quad (25)$$

For the hadronization temperature $T_H = 156$ MeV, this ratio is 1.020. The estimated multiplicities for D^{*0} and D^{*+} are

$$(dN_{D^{*0}}/dy)_0 = 2.57, \quad (dN_{D^{*+}}/dy)_0 = 2.52. \quad (26)$$

The SHM predictions for the multiplicities for D^0 and D^+ take into account D^* decays. We obtain the predictions for the multiplicities before D^* decays by using Eqs. (9) with $B_{+0} = 67.7\%$:

$$(dN_{D^0}/dy)_0 = 2.14, \quad (dN_{D^+}/dy)_0 = 2.03. \quad (27)$$



FIG. 1. One-loop Feynman diagrams for the D self-energy in HH χ EFT. The D , D^* , and π are represented by solid, double (solid+dashed), and dashed lines, respectively.

The ratio of a charm-meson multiplicity in Eqs. (26) or (27) to the pion multiplicity in Eq. (22) can be identified with the ratio of the charm-meson number density to the pion number density at kinetic freezeout

$$\frac{(dN_{D^{(*)}a}/dy)_0}{dN_\pi/dy} = \frac{\mathbf{n}_{D^{(*)}a}(\tau_{\text{kf}})}{\mathbf{n}_\pi(\tau_{\text{kf}})}. \quad (28)$$

IV. MASS SHIFTS AND THERMAL WIDTHS

In this section, we determine the mass shifts and thermal widths of pions and charm mesons in a hadron gas at temperatures near that of kinetic freezeout. The dominant effects from the hadronic medium come from coherent pion forward scattering.

A. Coherent pion forward scattering

When a particle propagates through a medium, its properties are modified by the interactions with the medium. The modifications can be described by the self-energy $\Pi(p)$, which depends on the energy and momentum of the particle and also on the properties of the medium. The real part of $\Pi(p)$ at $\mathbf{p} = 0$ determines the shift in the rest mass of the particle. The imaginary part of $\Pi(p)$ at $\mathbf{p} = 0$ determines the thermal width of the particle at rest.

If the particle is in thermal equilibrium with the medium, its self-energy can be calculated using thermal field theory. To be more specific, we consider the self-energy $\Pi_D(p)$ of a pseudoscalar charm meson D . The one-loop Feynman diagrams for $\Pi_D(p)$ in HH χ EFT are shown in Fig. 1. The first diagram can be expressed as the sum of a vacuum contribution and a thermal contribution from pions. The second diagram can be expressed as the sum of a vacuum contribution, a thermal contribution from pions, and a thermal contribution from vector charm mesons D^* . At temperatures relevant to the hadron gas, thermal contributions from vector charm mesons are severely suppressed by a Boltzmann factor $\exp(-M_*/T)$. The thermal contributions from pions can be expressed as an integral over the pion momentum \mathbf{q} weighted by the Bose-Einstein distribution $1/(e^{\beta\omega_q} - 1)$, where $\omega_q = \sqrt{m_\pi^2 + q^2}$.

The thermal contribution from pions to the D self-energy can be calculated alternatively from the tree diagrams for πD scattering in Fig. 2. At this order, the thermal contribution from pions comes from coherent pion forward scattering. If a pion with flavor k and momentum \mathbf{q} is scattered back into the state with the same flavor k and momentum \mathbf{q} , the initial many-body state is the charm meson plus the medium (which includes the pion with flavor k and momentum \mathbf{q}), and the final many-body state is also the charm meson plus the medium. Since the initial state is the same for all \mathbf{q} and the final state is also the same, the

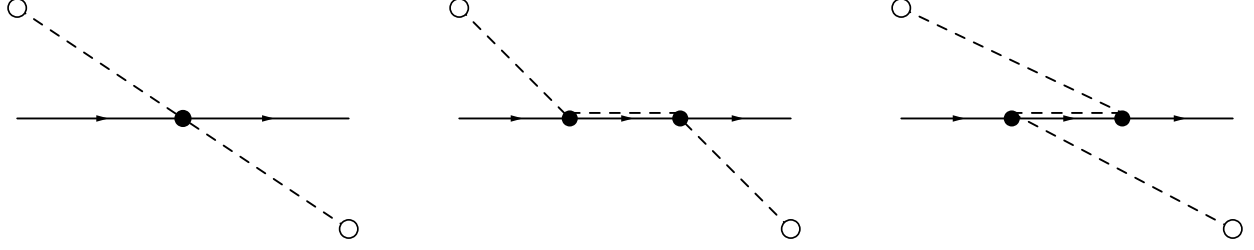


FIG. 2. Feynman diagrams for the D self-energy from coherent pion forward scattering in $\text{HH}\chi\text{EFT}$ at LO. The empty circles indicate an incoming and outgoing pion with the same flavor and the same 3-momentum. These diagrams can be obtained by cutting the pion lines in the diagrams in Fig. 1. The second diagram has a D^* resonance contribution.

pion-forward-scattering amplitudes must be added coherently for all momenta \mathbf{q} and all pion flavors k . The D self-energy from coherent pion forward scattering can be obtained from the negative of the \mathcal{T} -matrix element by weighting it by $\mathfrak{f}_\pi(\omega_q)/(2\omega_q)$, where $\mathfrak{f}_\pi(\omega_q)$ is the pion momentum distribution and $1/(2\omega_q)$ is a normalization factor, integrating over the pion momentum \mathbf{q} with measure $d^3q/(2\pi)^3$, and summing over the three pion flavors. If the pions are in chemical and thermal equilibrium at temperature T , the pion momentum distribution is the Bose-Einstein distribution in Eq. (18). However, this prescription for the self-energy from coherent pion forward scattering applies equally well to any medium in which the pions have a momentum distribution $\mathfrak{f}_\pi(\omega_q)$.

The thermal contribution from pions to the D self-energy can be obtained directly from the D self-energy diagrams in Fig. 1 by making a simple substitution for the pion propagator in the loop:

$$\frac{i}{q^2 - m_\pi^2 + i\epsilon} \longrightarrow \mathfrak{f}_\pi(|q_0|) 2\pi\delta(q^2 - m_\pi^2). \quad (29)$$

The delta function can be expressed as

$$\delta(q^2 - m_\pi^2) = \sum_{\pm} \theta(\pm q_0) \frac{1}{2\omega_q} \delta(|q_0| - \omega_q). \quad (30)$$

This substitution is referred to as the cutting of the pion line. The cutting of the pion line in the first diagram in Fig. 1 is 0, because the vertex is 0 when the incoming and outgoing pions have the same flavor. The cutting of the pion line in the second diagram in Fig. 1 gives the last two forward-scattering diagrams in Fig. 2. They come from the positive and negative regions of q_0 , respectively.

B. Pions

The thermal mass shift and the thermal width for a pion in a pion gas can be calculated using χEFT . The mass shift for a pion in thermal equilibrium was first calculated using χEFT at LO by Gasser and Leutwyler [27]. The pion thermal width was calculated in the low-density limit using χEFT at NLO by Goity and Leutwyler [28]. A complete calculation of the self-energy of a pion in thermal equilibrium in χEFT at NLO was presented by Schenk

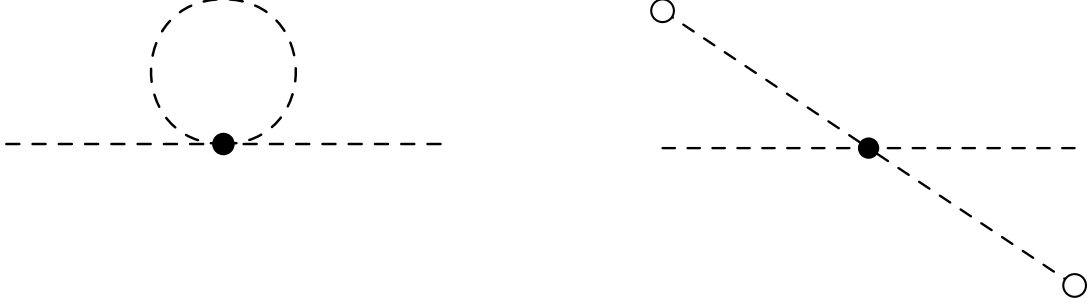


FIG. 3. One-loop Feynman diagram for the pion self-energy in χ EFT at LO (left panel) and the corresponding Feynman diagram for the pion self-energy from coherent pion forward scattering (right panel).

[29]. It was used to obtain the pion mass shift and the pion thermal width. The pion mass shift at NLO has also been calculated by Toublan [30].

The pion self-energy in χ EFT at LO is given by the one-loop Feynman diagram in the left panel of Fig. 3. The thermal contribution to the pion self-energy can also be obtained from the Feynman diagram for coherent pion forward scattering in the right panel of Fig. 3. The self-energy $\Pi_\pi(p_0, p)$ of a pion with 4-momentum (p_0, \mathbf{p}) can be obtained from the negative of the amplitude $\mathcal{A}_{ik,jk}(p_0, \mathbf{p}, \mathbf{q})$ for forward scattering of an on-shell pion with flavor k and 3-momentum \mathbf{q} by weighting it by $\mathfrak{f}_\pi(\omega_q)/(2\omega_q)$, integrating over \mathbf{q} , and summing over the three pion flavors k :

$$\Pi_\pi(p_0, p) \delta^{ij} = - \sum_k \int \frac{d^3q}{(2\pi)^3 2\omega_q} \mathfrak{f}_\pi(\omega_q) \mathcal{A}_{ik,jk}(p_0, \mathbf{p}, \mathbf{q}). \quad (31)$$

The amplitude $\mathcal{A}_{ik,jk}$ at LO does not depend on \mathbf{q} :

$$\mathcal{A}_{ik,jk}(p_0, p) = -\frac{2}{3f_\pi^2} [(2p_0^2 - 2p^2 + m_\pi^2) \delta^{ij} - 2(p_0^2 - p^2 + 2m_\pi^2) \delta^{ik} \delta^{jk}]. \quad (32)$$

The pion self-energy at LO is

$$\Pi_\pi(p_0, p) = \frac{1}{3f_\pi^2} (4p_0^2 - 4p^2 - m_\pi^2) \mathbf{n}_\pi \left\langle \frac{1}{\omega_q} \right\rangle_{\mathbf{q}}, \quad (33)$$

where the angular brackets represents the average over the Bose-Einstein distribution for the pion defined in Eq. (21).

The pion mass shift δm_π and the thermal width Γ_π can be obtained by evaluating the pion self-energy on the mass shell at zero 3-momentum:

$$\Pi_\pi(p_0 = m_\pi, p = 0) = 2m_\pi \delta m_\pi - i m_\pi \Gamma_\pi. \quad (34)$$

The pion mass shift in χ EFT at LO is

$$\delta m_\pi = \frac{m_\pi}{2f_\pi^2} \mathbf{n}_\pi \left\langle \frac{1}{\omega_q} \right\rangle_{\mathbf{q}}. \quad (35)$$

The pion thermal width Γ_π is 0 in χ EFT at LO. In a pion gas in chemical and thermal equilibrium at the temperature $T_{\text{kf}} = 115$ MeV, the pion mass shift is 1.55 MeV.

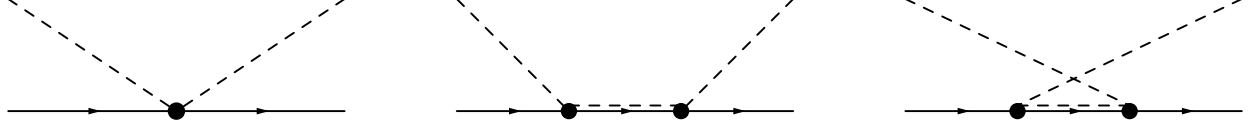


FIG. 4. Feynman diagrams for $\pi D \rightarrow \pi D$ in $\text{HH}\chi\text{EFT}$ at LO. The second diagram has a D^* resonance contribution.

C. Pseudoscalar charm mesons

The contributions to the thermal mass shift and thermal width of a pseudoscalar charm meson in a pion gas from coherent pion forward scattering can be calculated using $\text{HH}\chi\text{EFT}$.

1. D self-energy

In $\text{HH}\chi\text{EFT}$ at LO, the reaction $\pi D \rightarrow \pi D$ proceeds through the three diagrams in Fig. 4. The 4-momentum of D can be expressed as $P = Mv + p$, where v is the velocity 4-vector and p is the residual 4-momentum. The amplitude for the transition $D^a(p)\pi^i(q) \rightarrow D^b(p')\pi^j(q')$ is

$$\mathcal{A}_{ai,bj}(p, q, q') = \frac{1}{2f_\pi^2} [\sigma^i, \sigma^j]_{ab} v \cdot (q + q') - \frac{g_\pi^2}{f_\pi^2} \left((\sigma^i \sigma^j)_{ab} \frac{-q \cdot q' + (v \cdot q)(v \cdot q')}{v \cdot (p + q) - \Delta + i\Gamma_*/2} + (\sigma^j \sigma^i)_{ab} \frac{-q \cdot q' + (v \cdot q)(v \cdot q')}{v \cdot (p - q') - \Delta + i\Gamma_*/2} \right). \quad (36)$$

We have inserted the D^* width in the denominators to allow for the possibility that the D^* can be on shell. In the case of the forward scattering of $\pi^k(q)$ to $\pi^k(q)$, the amplitude reduces to a function of $v \cdot p$ and $v \cdot q$ and it is diagonal in a and b . The diagonal entry is

$$\mathcal{A}_{ak,ak}(v \cdot p, v \cdot q) = -\frac{2g_\pi^2}{f_\pi^2} \frac{[(v \cdot q)^2 - m_\pi^2](\Delta - v \cdot p)}{(v \cdot q)^2 - (\Delta - v \cdot p)^2 + i(\Delta - v \cdot p)\Gamma_*}. \quad (37)$$

Since $\Gamma_* \ll \Delta$, we have omitted the terms proportional to Γ_* in the numerator and to Γ_*^2 in the denominator.

The D self energy $\Pi_D(v \cdot p)$ in $\text{HH}\chi\text{EFT}$ at LO is the sum of the two one-loop diagrams in Fig. 1. The contribution from coherent pion forward scattering is the sum of the three tree diagrams in Fig. 2. The coherent sum of the first diagram over pion flavors is 0. The D self energy can be obtained from the amplitude in Eq. (37) by multiplying it by $-1/2$, weighting it by $\mathfrak{f}_\pi(\omega_q)/(2\omega_q)$, integrating over the momentum \mathbf{q} , and summing over the three pion flavors k . We choose the velocity 4-vector v of the charm meson to be the same as the 4-vector that defines the thermal frame in which the pion momentum distribution is Eq. (18) before kinetic freezeout and Eq. (20) after kinetic freezeout. The pion energy is $v \cdot q = \omega_q$. The D self-energy is

$$\Pi_D(v \cdot p) = \frac{3g_\pi^2}{f_\pi^2} \int \frac{d^3q}{(2\pi)^3 2\omega_q} \mathfrak{f}_\pi(\omega_q) \frac{(\omega_q^2 - m_\pi^2)(\Delta - v \cdot p)}{\omega_q^2 - (\Delta - v \cdot p)^2 + i(\Delta - v \cdot p)\Gamma_*}. \quad (38)$$

Since the charm-meson mass difference $\Delta = M_* - M$ is approximately equal to the pion mass m_π , the self-energy is sensitive to isospin splittings when the D is close to the mass shell $v \cdot p = 0$. The isospin splittings can be taken into account by reintroducing a sum over the flavors c of the intermediate D^* . In the self energy in Eq. (38), the factor $\sum_k (\sigma^k \sigma^k)_{aa} = 3\delta_{aa}$ from the pion vertices is replaced by $\sum_k \sum_c (\sigma^k)_{ac} (\sigma^k)_{ca} = \sum_c (2 - \delta_{ac})$. The mass difference Δ is replaced by Δ_{ac} and the pion energy is replaced by $\omega_{caq} = \sqrt{m_{\pi ca}^2 + q^2}$. The D^a self energy is

$$\Pi_{D^a}(v \cdot p) = \frac{g_\pi^2}{f_\pi^2} \sum_c (2 - \delta_{ac}) \int \frac{d^3 q}{(2\pi)^3 2\omega_{caq}} \mathfrak{f}_\pi(\omega_{caq}) \frac{q^2 (\Delta_{ca} - v \cdot p)}{\omega_{caq}^2 - (\Delta_{ca} - v \cdot p)^2 + i(\Delta_{ca} - v \cdot p)\Gamma_{*c}}, \quad (39)$$

where q^2 is the square of the 3-momentum.

2. Mass shift and thermal width

The mass shift δM_a and the thermal width $\delta \Gamma_a$ for the charm meson D^a in HH χ EFT at LO are obtained by evaluating the D^a self energy on the mass shell $v \cdot p = 0$:

$$\Pi_{D^a}(v \cdot p = 0) = \delta M_a - i \delta \Gamma_a / 2. \quad (40)$$

The D^a self energy with isospin splittings in Eq. (39) evaluated on the mass shell is

$$\Pi_{D^a}(0) = \frac{g_\pi^2}{f_\pi^2} \sum_c (2 - \delta_{ac}) \Delta_{ca} \int \frac{d^3 q}{(2\pi)^3 2\omega_{caq}} \mathfrak{f}_\pi(\omega_{caq}) \frac{q^2}{q^2 - q_{ca}^2 + i\Delta_{ca}\Gamma_{*c}}, \quad (41)$$

where $q_{ca}^2 = \Delta_{ca}^2 - m_{\pi ca}^2$. Since $\Delta_{ca}\Gamma_{*c} \ll |q^2 - q_{ca}^2|$ except in a very narrow range of q^2 , the expressions for δM_a and $\delta \Gamma_a$ can be simplified by taking the limit $\Gamma_{*c} \rightarrow 0$. The D^a mass shift in the limit $\Gamma_{*c} \rightarrow 0$ can be expressed in terms of an average over the pion momentum distribution of a function of q that involves a principal-value distribution:

$$\delta M_a = \frac{g_\pi^2}{2f_\pi^2} \mathbf{n}_\pi \sum_c (2 - \delta_{ac}) \Delta_{ca} \left\langle \frac{q^2}{\omega_{caq}} \mathcal{P} \frac{1}{q^2 - q_{ca}^2} \right\rangle. \quad (42)$$

The principal value is necessary only if $\Delta_{ca} > m_{\pi ca}$. The D^a thermal width in the limit $\Gamma_{*c} \rightarrow 0$ can be evaluated analytically by using a delta function:

$$\delta \Gamma_a = \frac{g_\pi^2}{4\pi f_\pi^2} \sum_c (2 - \delta_{ac}) \mathfrak{f}_\pi(\Delta_{ca}) q_{ca}^3 \theta(\Delta_{ca} - m_{\pi ca}). \quad (43)$$

This thermal width comes from the second diagram in Fig. 2 with a D^* in the s channel. The contribution from an intermediate D^{*c} is nonzero only if $\Delta_{ca} > m_{\pi ca}$. In a pion gas with temperature $T_{\text{kf}} = 115$ MeV, the mass shifts for D^+ and D^0 in Eq. (42) are $\delta M_+ = 1.269$ MeV and $\delta M_0 = 1.418$ MeV. The thermal widths for D^+ and D^0 in Eq. (43) are $\delta \Gamma_+ = 31.6$ keV and $\delta \Gamma_0 = 110.3$ keV.

The mass shift and thermal width of D^a can be expanded in powers of isospin splittings using the methods in Appendix B. The leading term in the expansion of the mass shift is the same for D^+ and D^0 :

$$\delta M \approx \frac{3g_\pi^2}{2f_\pi^2} \mathbf{n}_\pi m_\pi \left\langle \frac{1}{\omega_q} \right\rangle. \quad (44)$$

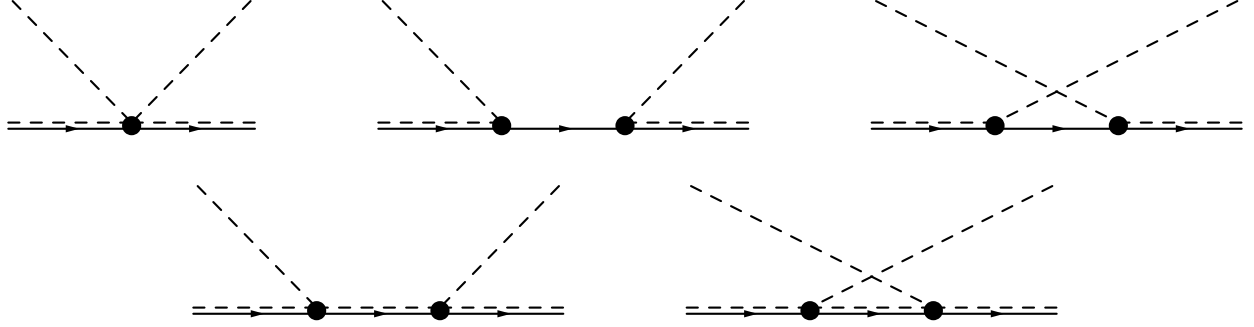


FIG. 5. Feynman diagrams for $\pi D^* \rightarrow \pi D^*$ in HH χ EFT at LO. The third diagram produces a D -meson t -channel singularity in the reaction rate.

The leading term in the expansion of the D^a thermal width is

$$\delta\Gamma_a \approx 3 \mathfrak{f}_\pi(m_\pi) \sum_c \Gamma[D^{*c} \rightarrow D^a \pi], \quad (45)$$

where $\Gamma[D^{*c} \rightarrow D^a \pi]$ is the partial decay rate of D^{*c} in Eq. (8). In a pion gas with temperature $T_{\text{kf}} = 115$ MeV, the D mass shift in Eq. (44) is $\delta M = 1.257$ MeV. The thermal widths for D^+ and D^0 in Eq. (45) are $\delta\Gamma_+ = 32.6$ keV and $\delta\Gamma_0 = 118.9$ keV.

D. Vector charm mesons

The contributions to the thermal mass shift and thermal width of a vector charm meson in a pion gas from coherent pion forward scattering can be calculated using HH χ EFT.

1. D^* self-energy

In HH χ EFT at LO, the reaction $\pi D^* \rightarrow \pi D^*$ proceeds through the five diagrams in Fig. 5. The 4-momentum of D^* can be expressed as $P = Mv + p$, where v is the velocity 4-vector and p is the residual 4-momentum. The amplitude for the transition $\pi^i(q) D^{*a}(p) \rightarrow \pi^j(q') D^{*b}(p')$ is

$$\begin{aligned} \mathcal{A}_{ai,bj}^{\mu\nu} = & -\frac{1}{2f_\pi^2} g^{\mu\nu} [\sigma^i, \sigma^j]_{ab} v \cdot (q + q') \\ & -\frac{g_\pi^2}{f_\pi^2} \left[(\sigma^i \sigma^j)_{ab} \frac{q^\mu q'^\nu}{v \cdot (p + q) + i\Gamma/2} + (\sigma^j \sigma^i)_{ab} \frac{q'^\mu q^\nu}{v \cdot (p - q') + i\Gamma/2} \right] \\ & +\frac{g_\pi^2}{f_\pi^2} \epsilon^{\mu\rho\lambda}(v) \epsilon^{\nu\sigma}{}_\lambda(v) \left[(\sigma^i \sigma^j)_{ab} \frac{q_\rho q'_\sigma}{v \cdot (p + q) - \Delta} + (\sigma^j \sigma^i)_{ab} \frac{q'_\rho q_\sigma}{v \cdot (p - q') - \Delta} \right], \quad (46) \end{aligned}$$

where $\epsilon^{\mu\rho\lambda}(v) = \epsilon^{\mu\rho\lambda\alpha} v_\alpha$. We have inserted the D width in the denominators of the D propagators to allow for the possibility that the D can be on shell. In the case of the forward

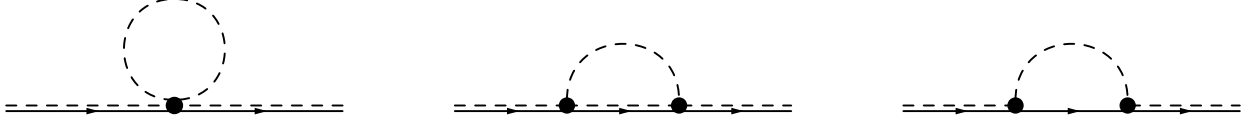


FIG. 6. One-loop Feynman diagrams for the D^* self-energy in $\text{HH}\chi\text{EFT}$.

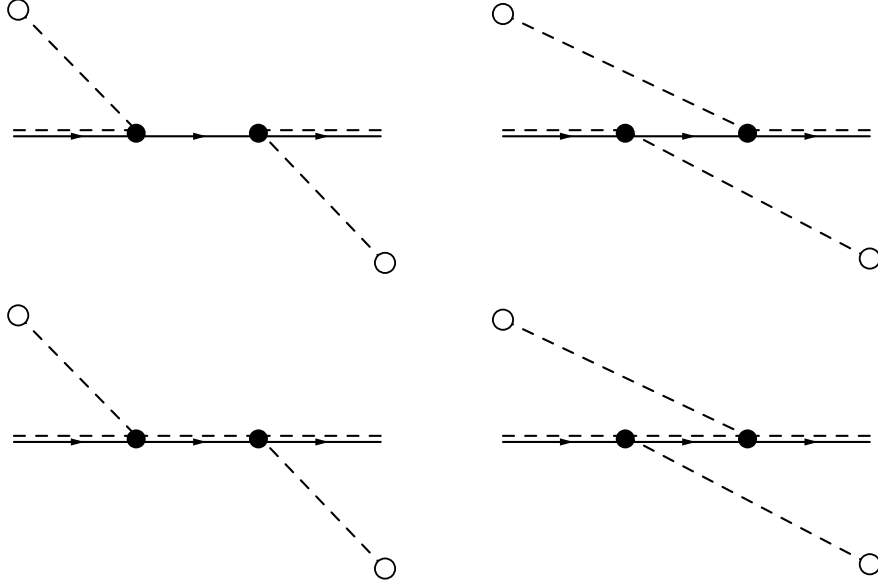


FIG. 7. Feynman diagrams for the D^* self energy from coherent pion forward scattering in $\text{HH}\chi\text{EFT}$ at LO. These diagrams can be obtained by cutting the pion lines in the last two diagrams in Fig. 6. The second diagram in the first row produces a D -meson t -channel singularity.

scattering of $\pi^k(q)$ to $\pi^k(q)$, the amplitude is diagonal in a and b . The diagonal entry is

$$\mathcal{A}_{ak,ak}^{\mu\nu} = \frac{2g_\pi^2}{f_\pi^2} \left[q^\mu q^\nu \frac{v \cdot p}{(v \cdot q)^2 - (v \cdot p)^2 - i v \cdot p \Gamma} - \epsilon^{\mu\lambda}(v, q) \epsilon^\nu{}_\lambda(v, q) \frac{v \cdot p - \Delta}{(v \cdot q)^2 - (\Delta - v \cdot p)^2} \right], \quad (47)$$

where $\epsilon^{\mu\lambda}(v, q) = \epsilon^{\mu\lambda\alpha\beta} v_\alpha q_\beta$. Since $\Gamma \ll \Delta$, we have omitted terms proportional to Γ in the numerator and to Γ^2 in the denominator.

The self-energy tensor $\Pi^{\mu\nu}$ of a vector meson D^* in $\text{HH}\chi\text{EFT}$ at LO is the sum of the three one-loop Feynman diagrams in Fig. 6. The contribution from coherent pion forward scattering can be obtained by cutting the pion lines using the prescription in Eq. (29). The cut of the first diagram in Fig. 6 is zero, because the coherent sum over pion flavors is 0. The cuts of the last two diagrams in Fig. 6 give the four tree diagrams in Fig. 7. By rotational symmetry, the contribution to $\Pi^{\mu\nu}$ from the coherent forward scattering of a pion with 4-momentum q is a linear combination of $g^{\mu\nu}$, $q^\mu q^\nu$, $v^\mu q^\nu + q^\mu v^\nu$, and $v^\mu v^\nu$. However the tensor structure of the D^* propagator in Eq. (A4) ensures that only the $-g^{\mu\nu} + v^\mu v^\nu$ component contributes to the D^* self energy $\Pi_{D^*}(v \cdot p)$. That component can be obtained from the tensor $\mathcal{A}_{ak,ak}^{\mu\nu}$ in Eq. (47) by contracting it with $(-g^{\mu\nu} + v^\mu v^\nu)/3$. The D^* self energy can

be obtained from that component by multiplying it by $-1/2$, weighting it by $f_\pi(\omega_q)/(2\omega_q)$, integrating over \mathbf{q} , and summing over the three pion flavors k :

$$\Pi_{D^*}(v \cdot p) = -\frac{g_\pi^2}{f_\pi^2} \int \frac{d^3q}{(2\pi)^3 2\omega_q} f_\pi(\omega_q) (\omega_q^2 - m_\pi^2) \left(\frac{v \cdot p}{\omega_q^2 - (v \cdot p)^2 - i v \cdot p \Gamma} + \frac{2(v \cdot p - \Delta)}{\omega_q^2 - (v \cdot p - \Delta)^2} \right). \quad (48)$$

Since the charm-meson mass difference $\Delta = M_* - M$ is approximately equal to the pion mass m_π , the self energy is sensitive to isospin splittings when the D^* is close to the mass shell $v \cdot p = \Delta$. The isospin splittings can be taken into account by reintroducing a sum over the flavors c of the intermediate D or D^* . In the self energy in Eq. (48), the factor $\sum_k (\sigma^k \sigma^k)_{aa} = 3\delta_{aa}$ from the pion vertices is replaced by $\sum_k \sum_c (\sigma^k)_{ac} (\sigma^k)_{ca} = \sum_c (2 - \delta_{ac})$. The isospin splittings in the denominators of the propagators can be taken into account in the first term in Eq. (48) by replacing $v \cdot p$ by $v \cdot p - M_c + M$ and Γ by Γ_c . They can be taken into account in the second term by replacing $v \cdot p - \Delta$ by $v \cdot p - M_{*c} + M$. The mass-shell condition $v \cdot p = \Delta$ is modified to $v \cdot p = M_{*a} - M$.

2. Mass shift and thermal width

The mass shift δM_{*a} and the thermal width $\delta \Gamma_{*a}$ for the charm meson D^{*a} in HH χ EFT at LO are obtained by evaluating the self-energy on the mass shell:

$$\Pi_{D^{*a}}(v \cdot p = \Delta) = \delta M_{*a} - i \delta \Gamma_{*a}/2. \quad (49)$$

If isospin splittings are taken into account in Eq. (48), the D^{*a} self-energy on the mass shell is

$$\Pi_{D^{*a}}(\Delta) = -\frac{g_\pi^2}{3f_\pi^2} \sum_c (2 - \delta_{ac}) \int \frac{d^3q}{(2\pi)^3 2\omega_{acq}} f_\pi(\omega_{acq}) \left(\frac{q^2 \Delta_{ac}}{q^2 - q_{ac}^2 - i \Delta_{ac} \Gamma_c} + \frac{2q^2 (M_{*a} - M_{*c})}{\omega_{acq}^2} \right), \quad (50)$$

where $\omega_{acq} = \sqrt{m_{\pi ac}^2 + q^2}$ and $q_{ac}^2 = \Delta_{ac}^2 - m_{\pi ac}^2$. In the second term inside the parentheses, we have omitted the term $-(M_{*a} - M_{*c})^2$ in the denominator, because $M_{*+} - M_{*0} \ll m_\pi$.

Since $\Delta_{ac} \Gamma_c \ll |q^2 - q_{ac}^2|$ except in a very narrow range of q^2 , the expressions for δM_{*a} and $\delta \Gamma_{*a}$ can be simplified by taking the limit $\Gamma_c \rightarrow 0$. The resulting D^{*a} mass shift is

$$\delta M_{*a} = -\frac{g_\pi^2}{6f_\pi^2} \mathbf{n}_\pi \sum_c (2 - \delta_{ac}) \left[\Delta_{ac} \left\langle \frac{q^2}{\omega_{acq}} \mathcal{P} \frac{1}{q^2 - q_{ac}^2} \right\rangle_{\mathbf{q}} + 2(M_{*a} - M_{*c}) \left\langle \frac{q^2}{\omega_{acq}^3} \right\rangle_{\mathbf{q}} \right]. \quad (51)$$

Note that the sum $\delta M_{*+} + \delta M_{*0}$ is equal to the sum $\delta M_+ + \delta M_0$ from Eq. (42) multiplied by $-1/3$. Thus the spin-weighted average of the D and D^* mass shifts is 0. The resulting D^{*a} thermal width can be evaluated analytically:

$$\delta \Gamma_{*a} = \frac{g_\pi^2}{12\pi f_\pi^2} \sum_c (2 - \delta_{ac}) f_\pi(\Delta_{ac}) q_{ac}^3 \theta(\Delta_{ac} - m_{\pi ac}). \quad (52)$$

This thermal width comes from the coherent pion forward scattering diagram with a D in the t channel in Fig. 7. Note that the sum $\delta\Gamma_{*+} + \delta\Gamma_{*0}$ is equal to the 1/3 of the sum $\delta\Gamma_{+} + \delta\Gamma_0$ from Eq. (45). In a pion gas with temperature $T_{\text{kf}} = 115$ MeV, the mass shifts for D^{*+} and D^{*0} are $\delta M_{*+} = -0.478$ MeV and $\delta M_{*0} = -0.417$ MeV. The thermal widths for D^{*+} and D^{*0} are $\delta\Gamma_{*+} = 32.7$ keV and $\delta\Gamma_{*0} = 14.6$ keV.

The mass shift and thermal width of D^{*a} can be expanded in powers of isospin splittings using the methods in Appendix B. The leading term in the expansion of the mass shift is the same for D^{*+} and D^{*0} and it differs from the mass shift δM for D^+ and D^0 in Eq. (44) by the multiplicative factor $-1/3$:

$$\delta M_* \approx -\delta M/3, \quad (53)$$

The leading term in the expansion of the D^{*a} thermal width is

$$\delta\Gamma_{*a} \approx f_\pi(m_\pi) \sum_c \Gamma[D^{*a} \rightarrow D^c\pi], \quad (54)$$

where $\Gamma[D^{*a} \rightarrow D^c\pi]$ is the D^* partial decay rate in Eq. (8). In a pion gas with temperature $T_{\text{kf}} = 115$ MeV, the D^* mass shift in Eq. (53) is $\delta M_* = -0.419$ MeV and the D^{*+} and D^{*0} thermal widths in Eq. (54) are $\delta\Gamma_{*+} = 35.2$ keV and $\delta\Gamma_{*0} = 15.3$ keV.

E. Expanding hadron gas

Thermal mass shifts and thermal widths have significant effects on some reaction rates for pions and charm mesons in the expanding hadron gas created by a heavy-ion collision. The pion mass shift δm_π in χ EFT at LO is given in Eq. (35). The charm-meson mass shifts δM_a for D^a and δM_{*a} for D^{*a} in HH χ EFT at LO are given in Eqs. (42) and (51). We will use the simpler approximations for the charm-meson mass shifts in Eqs. (44) and (53). The mass shifts in the hadron gas before kinetic freezeout are determined by the temperature T . The mass shifts after kinetic freezeout are determined by the pion number density \mathbf{n}_π . Some reaction rates are sensitive to mass differences through a factor of $M_* - M - m_\pi$ raised to a power. The four relevant mass differences in the vacuum are given in Eqs. (2). The thermal mass shifts for D^* , D , and π are given in Eqs. (53), (44), and (35). The mass differences in the hadron gas after kinetic freezeout decrease linearly with \mathbf{n}_π with the same slope:

$$\Delta_{00} - m_{\pi 0} \approx +7.04 \text{ MeV} - (3.23 \text{ MeV}) \mathbf{n}_\pi / \mathbf{n}_\pi^{(\text{kf})}, \quad (55a)$$

$$\Delta_{+0} - m_{\pi +} \approx +5.86 \text{ MeV} - (3.23 \text{ MeV}) \mathbf{n}_\pi / \mathbf{n}_\pi^{(\text{kf})}, \quad (55b)$$

$$\Delta_{++} - m_{\pi 0} \approx +5.63 \text{ MeV} - (3.23 \text{ MeV}) \mathbf{n}_\pi / \mathbf{n}_\pi^{(\text{kf})}, \quad (55c)$$

$$\Delta_{0+} - m_{\pi +} \approx -2.38 \text{ MeV} - (3.23 \text{ MeV}) \mathbf{n}_\pi / \mathbf{n}_\pi^{(\text{kf})}, \quad (55d)$$

where $\mathbf{n}_\pi^{(\text{kf})}$ is the pion number density at kinetic freezeout. The signs of the mass differences in Eqs. (55) imply that the decays $D^{*0} \rightarrow D^0\pi^0$, $D^{*+} \rightarrow D^+\pi^0$, and $D^{*+} \rightarrow D^+\pi^0$ are always kinematically allowed in the expanding hadron gas after kinetic freezeout, while the decay $D^{*0} \rightarrow D^+\pi^-$ is always forbidden.

The partial widths of the charm mesons from the decays $D^* \rightarrow D\pi$ are given in Eq. (8):

$$\Gamma_{D^{*+} \rightarrow D^+\pi} = \frac{g_\pi^2}{12\pi f_\pi^2} (\Delta_{++}^2 - m_{\pi 0}^2)^{3/2}. \quad (56a)$$

$$\Gamma_{D^{*+} \rightarrow D^0\pi} = \frac{g_\pi^2}{6\pi f_\pi^2} (\Delta_{+0}^2 - m_{\pi+}^2)^{3/2}, \quad (56b)$$

$$\Gamma_{D^{*0} \rightarrow D^0\pi} = \frac{g_\pi^2}{12\pi f_\pi^2} (\Delta_{00}^2 - m_{\pi 0}^2)^{3/2}, \quad (56c)$$

$$\Gamma_{D^{*0} \rightarrow D^+\pi} = 0, \quad (56d)$$

where $\Delta_{ab} = M_{*a} - M_b$ is the $D^{*a}-D^b$ mass difference. In the vacuum, the masses M_{*a} , M_b , and $m_{\pi ab}$ are constants. In the hadron gas, the mass shifts from coherent pion forward scattering can be taken into account by replacing Δ_{ab} in Eqs. (56) by $\Delta_{ab} + \delta M_* - \delta M$, where δM and δM_* are the charm-meson mass shifts in Eqs. (44) and (53), and replacing $m_{\pi i}$ by $m_{\pi i} + \delta m_\pi$, where δm_π is the pion mass shift in Eq. (35). In the expanding hadron gas after kinetic freezeout, the terms $\Delta_{ab}^2 - m_{\pi ab}^2$ in Eqs. (56) are quadratic functions of \mathbf{n}_π .

The thermal width Γ_a of D^a from coherent pion forward scattering is given in Eq. (45). The thermal widths for D^+ and D^0 are

$$\Gamma_+ = 3 \mathfrak{f}_\pi(m_\pi) \Gamma_{D^{*+} \rightarrow D^+\pi}, \quad (57a)$$

$$\Gamma_0 = 3 \mathfrak{f}_\pi(m_\pi) (\Gamma_{D^{*0} \rightarrow D^0\pi} + \Gamma_{D^{*+} \rightarrow D^0\pi}). \quad (57b)$$

In the hadron gas before kinetic freezeout, the factor $\mathfrak{f}_\pi(m_\pi)$ depends on the temperature T . In the hadron gas after kinetic freezeout at the temperature $T_{\text{kf}} = 115$ MeV, $\mathfrak{f}_\pi(m_\pi) = 0.431 \mathbf{n}_\pi / \mathbf{n}_\pi^{(\text{kf})}$, where $\mathbf{n}_\pi^{(\text{kf})}$ is the pion number density at kinetic freezeout. The thermal widths Γ_a in Eqs. (57) also depend on T or \mathbf{n}_π through the factors of $(\Delta_{ab}^2 - m_{\pi ab}^2)^{3/2}$ in $\Gamma_{D^{*a} \rightarrow D^b\pi}$.

The thermal correction $\delta\Gamma_{*a}$ to the width for D^{*a} is given in Eq. (54). The total widths for D^{*+} and D^{*0} are

$$\Gamma_{*+} = [1 + \mathfrak{f}_\pi(m_\pi)] (\Gamma_{D^{*+} \rightarrow D^+\pi} + \Gamma_{D^{*+} \rightarrow D^0\pi}) + \Gamma_{*+, \gamma}, \quad (58a)$$

$$\Gamma_{*0} = [1 + \mathfrak{f}_\pi(m_\pi)] \Gamma_{D^{*0} \rightarrow D^0\pi} + \Gamma_{*0, \gamma}, \quad (58b)$$

where $\Gamma_{*+, \gamma}$ and $\Gamma_{*0, \gamma}$ are the radiative decay rates in Eqs. (6). The terms with the factor $\mathfrak{f}_\pi(m_\pi)$ come from coherent pion forward scattering. In the hadron gas before kinetic freezeout, $\mathfrak{f}_\pi(m_\pi)$ depends on T . In the hadron gas after kinetic freezeout, $\mathfrak{f}_\pi(m_\pi) = 0.431 \mathbf{n}_\pi / \mathbf{n}_\pi^{(\text{kf})}$. The thermal widths Γ_{*a} in Eqs. (58) also depend on T or \mathbf{n}_π through the factors of $(\Delta_{ab}^2 - m_{\pi ab}^2)^{3/2}$ in $\Gamma_{D^{*a} \rightarrow D^b\pi}$.

The thermal widths for the charm mesons after kinetic freezeout at the temperature $T_{\text{kf}} = 115$ MeV are shown as functions of the pion number density \mathbf{n}_π in Fig. 8. The thermal widths of D^+ and D^0 are given in Eqs. (57). The thermal widths of D^{*+} and D^{*0} are given in Eqs. (58). The thicker curves in Fig. 8 take into account the thermal mass shifts of pions and charm mesons in the partial decay rates for $D^{*a} \rightarrow D^b\pi$ in Eqs. (56). The thinner straight lines in Fig. 8 are obtained by setting the masses of pions and charm mesons in those partial decay rates equal to their vacuum values. The effects of the thermal mass shifts are large. At kinetic freezeout, the thermal widths of D^+ and D^0 are 9.1 keV and 40.2 keV. As \mathbf{n}_π

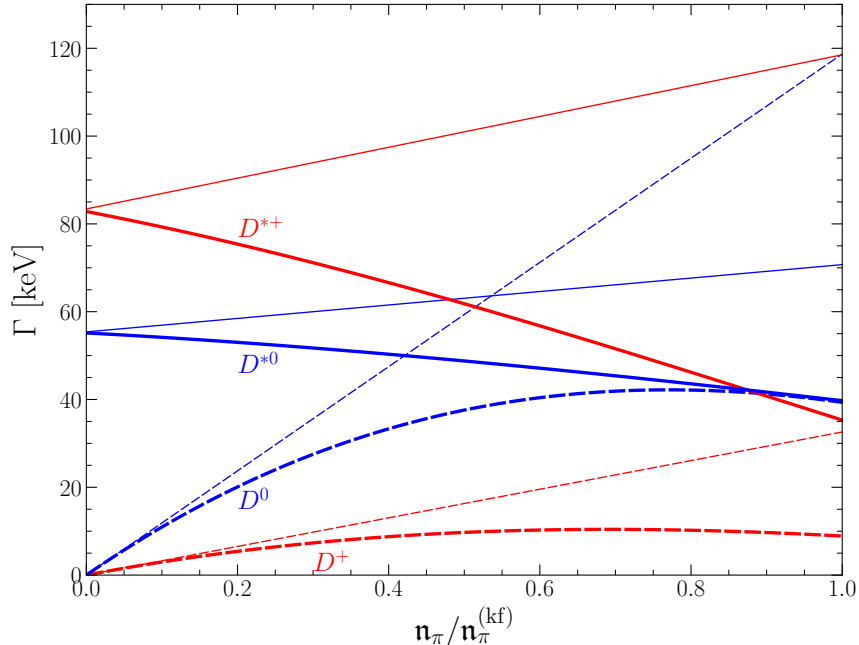


FIG. 8. Thermal widths for the charm mesons in the hadron gas after kinetic freezeout as functions of the pion number density \mathbf{n}_π : D^+ (dashed red), D^0 (dashed blue), D^{*+} (solid red), and D^{*0} (solid blue). The thicker curves include the effects of mass shifts from coherent pion forward scattering. The thinner straight lines ignore the thermal mass shifts.

decreases from $\mathbf{n}_\pi^{(\text{kf})}$ to 0, those decay rates increase to the maximum values 10.6 keV and 42.9 keV near $0.74 \mathbf{n}_\pi^{(\text{kf})}$ and then decrease to 0. At kinetic freezeout, the thermal widths of D^{*+} and D^{*0} are 35.6 keV and 39.9 keV. As \mathbf{n}_π decreases from $\mathbf{n}_\pi^{(\text{kf})}$ to 0, those decay rates increase to the vacuum values in Eqs. (5) to within errors. The decrease in the thermal widths of D^{*+} and D^{*0} with increasing \mathbf{n}_π may be counterintuitive, but it is a consequence of the decreasing phase space available for the decay because of the decreasing mass differences in Eqs. (55).

V. REACTION RATES

In this section, we calculate reaction rates for charm mesons in a pion gas. The results are applied to the hadron gas from a heavy-ion collision after kinetic freezeout.

A. $D^* \leftrightarrow D\pi$

The decays of D^* into $D\pi$ are 1-body reactions that give contributions to the rate equations for the number densities of D^* in a pion gas that are not suppressed by any powers of the pion number density. The partial decay rate in the vacuum for $D^{*a} \rightarrow D^b\pi$ in HH χ EFT at LO is given in Eq. (8). This rate is nonzero only if $\Delta_{ab} > m_{\pi ab}$, and it is sensitive to the masses through the factor of $(\Delta_{ab}^2 - m_{\pi ab}^2)^{3/2}$. This expression can also be used for the

partial decay rate in the pion gas by taking into account the mass shifts from coherent pion forward scattering. The charm-meson mass difference Δ_{ab} is shifted by $\delta M_* - \delta M$, where δM_* and δM are given by Eqs. (53) and (44). The pion mass $m_{\pi ab}$ is shifted by δm_π , which is given in Eq. (35).

The radiative decays of D^* into $D\gamma$ are also 1-body reactions. The partial decay rates for $D^* \rightarrow D\gamma$ in the vacuum are not sensitive to masses, because the D^* - D mass differences are much larger than the mass shifts. The radiative decay rates in the pion gas can therefore be approximated by their values in the vacuum in Eqs. (6).

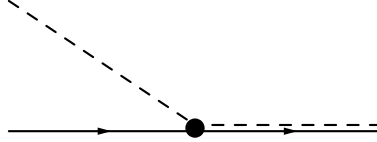


FIG. 9. Feynman diagram for $\pi D \rightarrow D^*$ in HH χ EFT at LO. The dashed line is a π , the solid line is a D , and the double (solid+dashed) line is a D^* .

A vector charm meson D^* can be produced in a pion gas by the inverse decay $\pi D \rightarrow D^*$. The reaction rate in the vacuum for $D^a \pi \rightarrow D^{*b}$ averaged over the three pion flavors is

$$v\sigma[\pi D^a \rightarrow D^{*b}] = \frac{\pi g_\pi^2}{6f_\pi^2} (2 - \delta_{ab}) \frac{q_{ba}^2}{\Delta_{ba}} \delta(\omega_{baq} - \Delta_{ba}), \quad (59)$$

$\omega_{baq} = \sqrt{m_{\pi ba}^2 + q^2}$, and $q_{ba}^2 = \Delta_{ba}^2 - m_{\pi ba}^2$. The reaction rate in the pion gas is obtained by averaging over the momentum distributions of the incoming D and π . The average over the D momentum distribution has no effect, because the reaction rate in Eq. (59) does not depend on the charm-meson momentum. The average over the pion momentum distribution can be evaluated using the delta function in Eq. (59):

$$\langle v\sigma[\pi D^a \rightarrow D^{*b}] \rangle = (\mathbf{f}_\pi(\Delta_{ba})/\mathbf{n}_\pi) \Gamma[D^{*b} \rightarrow D^a \pi], \quad (60)$$

where $\Gamma[D^{*b} \rightarrow D^a \pi]$ is the decay rate in Eq. (8). Since Δ_{ba} is large compared to isospin splittings, it can be approximated by the average Δ over the four $D^{*b} \rightarrow D^a \pi$ transitions or alternatively by the pion mass m_π . The reaction rates for $\pi D^a \rightarrow D^{*b}$ in the hadron gas near or after kinetic freezeout are

$$\langle v\sigma_{\pi D^+ \rightarrow D^{*+}} \rangle = [\mathbf{f}_\pi(m_\pi)/\mathbf{n}_\pi] \Gamma_{D^{*+} \rightarrow D^+ \pi}, \quad (61a)$$

$$\langle v\sigma_{\pi D^0 \rightarrow D^{*+}} \rangle = [\mathbf{f}_\pi(m_\pi)/\mathbf{n}_\pi] \Gamma_{D^{*+} \rightarrow D^0 \pi}, \quad (61b)$$

$$\langle v\sigma_{\pi D^0 \rightarrow D^{*0}} \rangle = [\mathbf{f}_\pi(m_\pi)/\mathbf{n}_\pi] \Gamma_{D^{*0} \rightarrow D^0 \pi}, \quad (61c)$$

$$\langle v\sigma_{\pi D^+ \rightarrow D^{*0}} \rangle = 0. \quad (61d)$$

Before kinetic freezeout, the factor $\mathbf{f}_\pi(m_\pi)/\mathbf{n}_\pi$ is determined by the temperature T . After kinetic freezeout at the temperature $T_{\text{kf}} = 115$ MeV, that factor has the constant value $0.431/\mathbf{n}_\pi^{(\text{kf})}$ independent of \mathbf{n}_π .

B. $\pi D \rightarrow \pi D$

The reaction $\pi D^a \rightarrow \pi D^b$ can change the flavor of a pseudoscalar charm meson. The Feynman diagrams for this reaction in HH χ EFT at LO are shown in Fig. 4. The reaction rate has a D^* resonance contribution from the second diagram in Fig. 4 that is sensitive to isospin splittings and to the D^* width. A simple expression for the nonresonant contribution to the reaction rate can be obtained by setting the D^*-D mass splitting Δ equal to the pion mass m_π and then taking the limit as the D^* width Γ_* approaches 0. A simple expression for the resonant contribution to the reaction rate can be obtained by isolating the term with the factor $1/\Gamma_*$. We approximate the reaction rate by the sum of the nonresonant reaction rate and the resonant reaction rate.

The \mathcal{T} -matrix element for $\pi^i D^a \rightarrow \pi^j D^b$ in the zero-width limit is obtained from the amplitude in Eq. (36) by setting $\Gamma_* = 0$ and by putting the external legs on shell by setting $v \cdot p = 0$, $v \cdot q = \omega_q$, and $v \cdot q' = \omega_{q'}$:

$$\mathcal{T}_{ai,bj} = \frac{1}{2f_\pi^2} [\sigma^i, \sigma^j]_{ab} (\omega_q + \omega_{q'}) - \frac{g_\pi^2}{f_\pi^2} \left[(\sigma^i \sigma^j)_{ab} \frac{\mathbf{q} \cdot \mathbf{q}'}{\omega_q - \Delta} - (\sigma^j \sigma^i)_{ab} \frac{\mathbf{q} \cdot \mathbf{q}'}{\omega_{q'} + \Delta} \right]. \quad (62)$$

We can ignore the recoil of D and set $|\mathbf{q}'| = |\mathbf{q}|$. The non-resonant reaction rate can be obtained by taking the limit $\Delta \rightarrow m_\pi$. The non-resonant reaction rate for $\pi D^a \rightarrow \pi D^b$ averaged over incoming pion flavors is

$$v\sigma[\pi D^a \rightarrow \pi D^b]_{\text{nonres}} = \frac{1}{12\pi f_\pi^4} [2(2 - \delta_{ab})(1 + g_\pi^4/3)\omega_q^2 + \delta_{ab} g_\pi^4 m_\pi^2] \frac{q}{\omega_q}, \quad (63)$$

where q is the 3-momentum of the incoming pion. The reaction rate in the pion gas can be obtained by averaging over the momentum distributions of the incoming D and π :

$$\langle v\sigma[\pi D^a \rightarrow \pi D^b]_{\text{nonres}} \rangle = \frac{1}{12\pi f_\pi^4} \left[2(2 - \delta_{ab})(1 + g_\pi^4/3) \langle \omega_q q \rangle_{\mathbf{q}} + \delta_{ab} g_\pi^4 m_\pi^2 \left\langle \frac{q}{\omega_q} \right\rangle_{\mathbf{q}} \right], \quad (64)$$

where the angular brackets represents the average over the Bose-Einstein distribution for the pion defined in Eq. (21).

The second diagram in Fig. 4 with D^{*c} in the s channel gives a resonance contribution to the reaction rate proportional to $1/\Gamma_{*c}$ if $\Delta_{ac} > m_{\pi ac}$. In the square of the matrix element for the scattering of a D with momentum $Mv + p$ and a π with momentum q , the resonance contribution can be isolated by making a simple substitution for the product of the D^* propagator and its complex conjugate:

$$\frac{1}{v \cdot (p + q) - \Delta + i\Gamma_{*c}/2} \left(\frac{1}{v \cdot (p + q) - \Delta + i\Gamma_{*c}/2} \right)^* \longrightarrow \frac{2\pi}{\Gamma_{*c}} \delta(v \cdot (p + q) - \Delta). \quad (65)$$

The resonant reaction rate for $\pi D^a \rightarrow \pi D^b$ averaged over the flavors of the incoming pion is

$$v\sigma[\pi D^a \rightarrow \pi D^b]_{\text{res}} = \frac{g_\pi^4}{72f_\pi^4} \sum_c (2 - \delta_{ac})(2 - \delta_{bc}) \frac{q_{ca}^2 q_{cb}^3}{\Delta_{ca} \Gamma_{*c}} \theta(\Delta_{cb} - m_{\pi cb}) \delta(\omega_{caq} - \Delta_{ca}), \quad (66)$$

where q is the 3-momentum of the incoming pion. Using the expressions for $\Gamma[D^* \rightarrow D\pi]$ in Eq. (8) and $v\sigma[\pi D \rightarrow D^*]$ in Eq. (59), the singular term in the reaction rate can be expressed as

$$v\sigma[\pi D^a \rightarrow \pi D^b]_{\text{res}} = \sum_c \frac{1}{\Gamma_{*c}} v\sigma[\pi D^a \rightarrow D^{*c}] \Gamma[D^{*c} \rightarrow D^b\pi]. \quad (67)$$

The reaction rate in the pion gas can be evaluated by using the thermal average of $v\sigma[\pi D \rightarrow D^*]$ in Eq. (60):

$$\langle v\sigma[\pi D^a \rightarrow \pi D^b]_{\text{res}} \rangle = \frac{f_\pi(\Delta)}{\mathbf{n}_\pi} \sum_c \frac{\Gamma[D^{*c} \rightarrow D^a\pi] \Gamma[D^{*c} \rightarrow D^b\pi]}{\Gamma_{*c}}. \quad (68)$$

The reaction rate for $\pi D^a \rightarrow \pi D^b$ in the pion gas can be approximated by the sum of the non-resonant reaction rate in Eq. (64) and the resonant reaction rate in Eq. (68). The reaction rates in the hadron gas near or after kinetic freezeout are

$$\langle v\sigma_{\pi D^0 \rightarrow \pi D^0} \rangle = (0.496 + 0.188 g_\pi^4) \frac{m_\pi^2}{f_\pi^4} + \frac{f_\pi(m_\pi)}{\mathbf{n}_\pi} \left(\frac{\Gamma_{D^{*0} \rightarrow D^0\pi}^2}{\Gamma_{*0}} + \frac{\Gamma_{D^{*+} \rightarrow D^0\pi}^2}{\Gamma_{*+}} \right), \quad (69a)$$

$$\langle v\sigma_{\pi D^0 \rightarrow \pi D^+} \rangle = (0.991 + 0.330 g_\pi^4) \frac{m_\pi^2}{f_\pi^4} + \frac{f_\pi(m_\pi)}{\mathbf{n}_\pi} \frac{\Gamma_{D^{*+} \rightarrow D^0\pi} \Gamma_{D^{*+} \rightarrow D^+\pi}}{\Gamma_{*+}}, \quad (69b)$$

$$\langle v\sigma_{\pi D^+ \rightarrow \pi D^0} \rangle = (0.991 + 0.330 g_\pi^4) \frac{m_\pi^2}{f_\pi^4} + \frac{f_\pi(m_\pi)}{\mathbf{n}_\pi} \frac{\Gamma_{D^{*+} \rightarrow D^0\pi} \Gamma_{D^{*+} \rightarrow D^+\pi}}{\Gamma_{*+}}, \quad (69c)$$

$$\langle v\sigma_{\pi D^+ \rightarrow \pi D^+} \rangle = (0.496 + 0.188 g_\pi^4) \frac{m_\pi^2}{f_\pi^4} + \frac{f_\pi(m_\pi)}{\mathbf{n}_\pi} \frac{\Gamma_{D^{*+} \rightarrow D^+\pi}^2}{\Gamma_{*+}}. \quad (69d)$$

The dimensionless numbers in the first terms depend only on m_π/T , which we have evaluated at $T_{\text{kf}} = 115$ MeV. Before kinetic freezeout, the factor $f_\pi(m_\pi)/\mathbf{n}_\pi$ is determined by T . After kinetic freezeout at $T_{\text{kf}} = 115$ MeV, that factor has the constant value $0.431/\mathbf{n}_\pi^{(\text{kf})}$ independent of \mathbf{n}_π . There can also be dependence on T or \mathbf{n}_π through the mass shifts in $\Gamma_{D^{*a} \rightarrow D^b\pi}$ and through the factors of $1/\Gamma_{*c}$.

The D^* resonance terms in the reaction rates for $\pi D^a \rightarrow \pi D^b$ in Eqs. (69) can be obtained from the reaction rates for $\pi D^a \rightarrow D^{*c}$ from Eqs. (61) by multiplying by the branching fraction $\Gamma_{D^{*c} \rightarrow D^b\pi}/\Gamma_{*c}$ and summing over the two flavors of D^{*c} . Thus if the reaction rates for $\pi D \rightarrow D^*$ in Eqs. (61) and $\pi D \rightarrow \pi D$ in Eqs. (69) are both included in a rate equation, the contributions of $\pi D \rightarrow D^*$ in which D^* subsequently decays to $D\pi$ are double counted. The only contributions of $\pi D \rightarrow D^*$ that are not double counted are those in which D^* subsequently decays to $D\gamma$. The double counting can be avoided by replacing the reaction rates for $\pi D \rightarrow D^*$ in Eqs. (61) by the contributions from the subsequent radiative decay of D^* :

$$\langle v\sigma_{\pi D^+ \rightarrow D^+\gamma} \rangle = [f_\pi(m_\pi)/\mathbf{n}_\pi] \Gamma_{D^{*+} \rightarrow D^+\pi} (\Gamma_{*+, \gamma}/\Gamma_{*+}), \quad (70a)$$

$$\langle v\sigma_{\pi D^0 \rightarrow D^+\gamma} \rangle = [f_\pi(m_\pi)/\mathbf{n}_\pi] \Gamma_{D^{*+} \rightarrow D^0\pi} (\Gamma_{*+, \gamma}/\Gamma_{*+}), \quad (70b)$$

$$\langle v\sigma_{\pi D^0 \rightarrow D^0\gamma} \rangle = [f_\pi(m_\pi)/\mathbf{n}_\pi] \Gamma_{D^{*0} \rightarrow D^0\pi} (\Gamma_{*0, \gamma}/\Gamma_{*0}), \quad (70c)$$

$$\langle v\sigma_{\pi D^+ \rightarrow D^0\gamma} \rangle = 0, \quad (70d)$$

where $\Gamma_{*+, \gamma}$ and $\Gamma_{*0, \gamma}$ are the radiative decay rates in the vacuum in Eqs. (6).

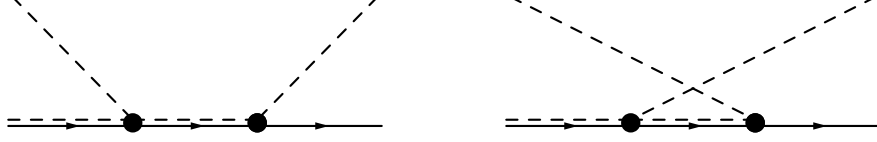


FIG. 10. Feynman diagrams for $\pi D^* \rightarrow \pi D$ in HH χ EFT at LO. The diagrams for $\pi D \rightarrow \pi D^*$ are the mirror images of these diagrams.

C. $\pi D^* \leftrightarrow \pi D$

The reactions $\pi D^* \leftrightarrow \pi D$ can change vector charm mesons into pseudoscalar charm mesons and vice versa. The reaction $\pi D^* \rightarrow \pi D$ is exothermic, releasing a mass energy comparable to m_π . Since this is large compared to isospin splittings, isospin splittings can be neglected. Relatively simple expressions for the reaction rates can be obtained by taking the limit $\Delta \rightarrow m_\pi$. The square of the matrix element for $\pi(q)D^{*a} \rightarrow \pi(q')D^b$ averaged over D^* spins and averaged/summed over pion flavors is

$$\overline{|\mathcal{M}|^2} = \frac{g_\pi^4}{9f_\pi^4} \frac{(\mathbf{q} \times \mathbf{q}')^2}{\omega_q^2 \omega_{q'}^2} [2(2 - \delta_{ab})(\omega_q - \omega_{q'})^2 + 3\delta_{ab}(\omega_q + \omega_{q'})^2]. \quad (71)$$

The reaction rate can be reduced to

$$v\sigma[\pi D^{*a} \rightarrow \pi D^b] = \frac{g_\pi^4}{216\pi f_\pi^4} \frac{q^2 [(\omega_q + \Delta)^2 - m_\pi^2]^{3/2}}{\omega_q^3 (\omega_q + \Delta)^2} [3\delta_{ab}(2\omega_q + \Delta)^2 + 2(2 - \delta_{ab})\Delta^2]. \quad (72)$$

The reaction rate in the pion gas in the limit $\Delta \rightarrow m_\pi$ is

$$\langle v\sigma[\pi D^{*a} \rightarrow \pi D^b] \rangle = \frac{g_\pi^4}{216\pi f_\pi^4} \left\langle \frac{q^2}{(\omega_q + m_\pi)^2} \left(\frac{\omega_q + 2m_\pi}{\omega_q} \right)^{3/2} \times [3\delta_{ab}(2\omega_q + m_\pi)^2 + 2(2 - \delta_{ab})m_\pi^2] \right\rangle_{\mathbf{q}}. \quad (73)$$

The square of the matrix element for $\pi D^a \rightarrow \pi D^{*b}$ summed over D^* spins and averaged/summed over the pion flavors can be obtained from $\overline{|\mathcal{M}|^2}$ for $\pi D^{*a} \rightarrow \pi D^b$ in Eq. (71) by multiplying by 3. The reaction rate in the pion gas in the limit $\Delta \rightarrow m_\pi$ is

$$\langle v\sigma[\pi D^a \rightarrow \pi D^{*b}] \rangle = \frac{g_\pi^4}{72\pi f_\pi^4} \left\langle \frac{q^2}{(\omega_q - m_\pi)^2} \left(\frac{\omega_q - 2m_\pi}{\omega_q} \right)^{3/2} \times [3\delta_{ab}(2\omega_q - m_\pi)^2 + 2(2 - \delta_{ab})m_\pi^2] \theta(\omega_q - 2m_\pi) \right\rangle_{\mathbf{q}}. \quad (74)$$

The theta function restricts the pion energy to be above the threshold $2m_\pi$ for producing πD^* , which requires $q > \sqrt{3}m_\pi$.

The reaction rates for $\pi D^a \rightarrow \pi D^{*b}$ in the hadron gas after kinetic freezeout are

$$\langle v\sigma_{\pi D^0 \rightarrow \pi D^{*0}} \rangle = \langle v\sigma_{\pi D^+ \rightarrow \pi D^{*+}} \rangle = 0.215 g_\pi^4 m_\pi^2 / f_\pi^4, \quad (75a)$$

$$\langle v\sigma_{\pi D^0 \rightarrow \pi D^{*+}} \rangle = \langle v\sigma_{\pi D^+ \rightarrow \pi D^{*0}} \rangle = 0.005 g_\pi^4 m_\pi^2 / f_\pi^4. \quad (75b)$$

The reaction rates for $\pi D^{*a} \rightarrow \pi D^b$ in the hadron gas after kinetic freezeout are

$$\langle v\sigma_{\pi D^{*0} \rightarrow \pi D^0} \rangle = \langle v\sigma_{\pi D^{*+} \rightarrow \pi D^+} \rangle = 0.243 g_\pi^4 m_\pi^2 / f_\pi^4, \quad (76a)$$

$$\langle v\sigma_{\pi D^{*0} \rightarrow \pi D^+} \rangle = \langle v\sigma_{\pi D^{*+} \rightarrow \pi D^0} \rangle = 0.006 g_\pi^4 m_\pi^2 / f_\pi^4. \quad (76b)$$

The dimensionless numerical factors depend only on m_π/T , which has been evaluated at $T_{\text{kf}} = 115$ MeV.

D. $\pi D^* \rightarrow \pi D^*$

The reaction $\pi D^* \rightarrow \pi D^*$ can change the flavor of a vector charm meson. The five Feynman diagrams for this reaction in HH χ EFT at LO are shown in Fig. 5. The third diagram, which proceeds through an intermediate D , produces a t -channel singularity in the reaction rate that is proportional to $1/\Gamma$ in the limit $\Gamma \rightarrow 0$. The singularity comes from the decay $D^* \rightarrow \pi D$ followed by the inverse decay $\pi D \rightarrow D^*$. A relatively simple expression for the nonsingular contribution to the reaction rate is obtained by setting $\Delta = m_\pi$ and then taking the limit $\Gamma \rightarrow 0$. A simple expression for the resonant contribution to the reaction rate can be obtained by isolating the term with the factor $1/\Gamma$. We approximate the reaction rate by the sum of the nonsingular reaction rate and the singular reaction rate.

The \mathcal{T} -matrix element for $\pi^i D^{*a} \rightarrow \pi^j D^{*b}$ in the zero-width limit is obtained from the amplitude in Eq. (46) by contracting it with the D^* polarization vectors, setting $\Gamma = 0$, and then putting the external legs on shell by setting $v \cdot p = \Delta$, $v \cdot q = \omega_q$, and $v \cdot q' = \omega_{q'}$:

$$\begin{aligned} \varepsilon_\mu \mathcal{T}_{ai,bj}^{\mu\nu} \varepsilon'^*{}_\nu &= -\frac{1}{2f_\pi^2} [\sigma^i, \sigma^j]_{ab} (\omega_q + \omega_{q'}) (\boldsymbol{\varepsilon} \cdot \boldsymbol{\varepsilon}'^*) \\ &\quad - \frac{g_\pi^2}{f_\pi^2} \left[(\sigma^i \sigma^j)_{ab} \frac{(\boldsymbol{\varepsilon} \cdot \mathbf{q})(\mathbf{q}' \cdot \boldsymbol{\varepsilon}'^*)}{\omega_q + \Delta} - (\sigma^j \sigma^i)_{ab} \frac{(\boldsymbol{\varepsilon} \cdot \mathbf{q}')(\mathbf{q} \cdot \boldsymbol{\varepsilon}'^*)}{\omega_{q'} - \Delta} \right] \\ &\quad + \frac{g_\pi^2}{f_\pi^2} \left[(\sigma^i \sigma^j)_{ab} \frac{(\boldsymbol{\varepsilon} \times \mathbf{q}) \cdot (\mathbf{q}' \times \boldsymbol{\varepsilon}'^*)}{\omega_q} - (\sigma^j \sigma^i)_{ab} \frac{(\boldsymbol{\varepsilon} \times \mathbf{q}') \cdot (\mathbf{q} \times \boldsymbol{\varepsilon}'^*)}{\omega_{q'}} \right]. \end{aligned} \quad (77)$$

We can ignore the recoil of D^* and set $|\mathbf{q}'| = |\mathbf{q}|$. The non-singular contribution to the reaction rate can be obtained by taking the limit $\Delta \rightarrow m_\pi$. The reaction rate averaged over incoming pion flavors and incoming D^* spins is

$$\begin{aligned} v\sigma[\pi D^{*a} \rightarrow \pi D^{*b}]_{\text{nonsing}} &= \frac{1}{36\pi f_\pi^4} \left\{ (2 - \delta_{ab}) [6\omega_q^2 + 2g_\pi^4(m_\pi^2 + q^4/\omega_q^2)] \right. \\ &\quad \left. + \delta_{ab} g_\pi^4 (3\omega_q^2 + q^4/\omega_q^2) \right\} \frac{q}{\omega_q}. \end{aligned} \quad (78)$$

The reaction rate in the pion gas is obtained by averaging over the momentum distributions of the incoming D and π :

$$\begin{aligned} \langle v\sigma[\pi D^{*a} \rightarrow \pi D^{*b}]_{\text{nonsing}} \rangle &= \frac{1}{36\pi f_\pi^4} \left([6(2 - \delta_{ab}) + 2(2 + \delta_{ab})g_\pi^4] \langle \omega_q q \rangle_{\mathbf{q}} \right. \\ &\quad \left. - 4g_\pi^4 m_\pi^2 \left\langle \frac{q}{\omega_q} \right\rangle_{\mathbf{q}} + (4 - \delta_{ab}) g_\pi^4 m_\pi^4 \left\langle \frac{q}{\omega_q^3} \right\rangle_{\mathbf{q}} \right). \end{aligned} \quad (79)$$

The third diagram in Fig. 5 produces a t -channel singularity, because the intermediate D can be on shell. In the square of the matrix element for an incoming D^* with momentum $(M + \Delta)v + p$ and an outgoing pion with momentum q' , the t -channel singularity can be isolated by making a simple substitution for the product of the D propagator and its complex conjugate:

$$\frac{1}{v \cdot (\Delta v + p - q') + i\Gamma/2} \left(\frac{1}{v \cdot (\Delta v + p - q') + i\Gamma/2} \right)^* \rightarrow \frac{2\pi}{\Gamma} \delta(\Delta + v \cdot p - v \cdot q'). \quad (80)$$

The t -channel singularity contribution to the reaction rate for $\pi(q)D^{*a}(p) \rightarrow \pi(q')D^{*b}(p')$ averaged over incoming D^* spins and over incoming pion flavors is

$$v\sigma[\pi D^{*a} \rightarrow \pi D^{*b}]_{\text{sing}} = \frac{g_\pi^4}{72 f_\pi^4} \sum_c (2 - \delta_{ac})(2 - \delta_{bc}) \frac{q_{bc}^2 q_{ac}^3}{\Delta_{bc} \Gamma_c} \delta(\omega_{bcq} - \Delta_{bc}) \theta(\Delta_{ac} - m_{\pi ac}). \quad (81)$$

Using the expressions for $\Gamma[D^* \rightarrow D\pi]$ in Eq. (8) and $v\sigma[D\pi \rightarrow D^*]$ in Eq. (59), the singular term in the reaction rate can be expressed as

$$v\sigma[\pi D^{*a} \rightarrow \pi D^{*b}]_{\text{sing}} = \sum_c \frac{1}{\Gamma_c} \Gamma[D^{*a} \rightarrow D^c \pi] v\sigma[D^c \pi \rightarrow D^{*b}]. \quad (82)$$

The reaction rate in the pion gas can be evaluated using the thermal average of $v\sigma[D\pi \rightarrow D^*]$ in Eq. (60):

$$\langle v\sigma[\pi D^{*a} \rightarrow \pi D^{*b}]_{\text{sing}} \rangle = \frac{\mathfrak{f}_\pi(\Delta)}{\mathbf{n}_\pi} \sum_c \frac{\Gamma[D^{*a} \rightarrow D^c \pi] \Gamma[D^{*b} \rightarrow D^c \pi]}{\Gamma_c}. \quad (83)$$

This differs from the resonant term in the reaction rate for $\pi D \rightarrow \pi D$ in Eq. (68) in that the sum is over D flavors instead of D^* flavors and that the product of D^* partial decay rates is divided by a D decay rate Γ_c instead of a D^* decay rate Γ_{*c} .

The reaction rates for $\pi D^{*a} \rightarrow \pi D^{*b}$ in the hadron gas near or after kinetic freezeout can be approximated by the sum of the nonsingular reaction rates in Eq. (79) and the t -channel singularity reaction rate in Eq. (83):

$$\langle v\sigma_{\pi D^{*0} \rightarrow \pi D^{*0}} \rangle = (0.496 + 0.469 g_\pi^4) \frac{m_\pi^2}{f_\pi^4} + \frac{\mathfrak{f}_\pi(m_\pi)}{\mathbf{n}_\pi} \frac{\Gamma_{D^{*0} \rightarrow D^0 \pi}^2}{\Gamma_0}, \quad (84a)$$

$$\langle v\sigma_{\pi D^{*0} \rightarrow \pi D^{*+}} \rangle = (0.991 + 0.306 g_\pi^4) \frac{m_\pi^2}{f_\pi^4} + \frac{\mathfrak{f}_\pi(m_\pi)}{\mathbf{n}_\pi} \frac{\Gamma_{D^{*0} \rightarrow D^0 \pi} \Gamma_{D^{*+} \rightarrow D^0 \pi}}{\Gamma_0}, \quad (84b)$$

$$\langle v\sigma_{\pi D^{*+} \rightarrow \pi D^{*0}} \rangle = (0.991 + 0.306 g_\pi^4) \frac{m_\pi^2}{f_\pi^4} + \frac{\mathfrak{f}_\pi(m_\pi)}{\mathbf{n}_\pi} \frac{\Gamma_{D^{*0} \rightarrow D^0 \pi} \Gamma_{D^{*+} \rightarrow D^0 \pi}}{\Gamma_0}, \quad (84c)$$

$$\langle v\sigma_{\pi D^{*+} \rightarrow \pi D^{*+}} \rangle = (0.496 + 0.469 g_\pi^4) \frac{m_\pi^2}{f_\pi^4} + \frac{\mathfrak{f}_\pi(m_\pi)}{\mathbf{n}_\pi} \left(\frac{\Gamma_{D^{*+} \rightarrow D^0 \pi}^2}{\Gamma_0} + \frac{\Gamma_{D^{*+} \rightarrow D^+ \pi}^2}{\Gamma_+} \right). \quad (84d)$$

The dimensionless numbers in the first terms depend only on m_π/T , which we have evaluated at $T_{\text{kf}} = 115$ MeV. Before kinetic freezeout, the factor $\mathfrak{f}_\pi(m_\pi)/\mathbf{n}_\pi$ is determined by T . After kinetic freezeout at $T_{\text{kf}} = 115$ MeV, that factor has the constant value $0.431/\mathbf{n}_\pi^{(\text{kf})}$ independent

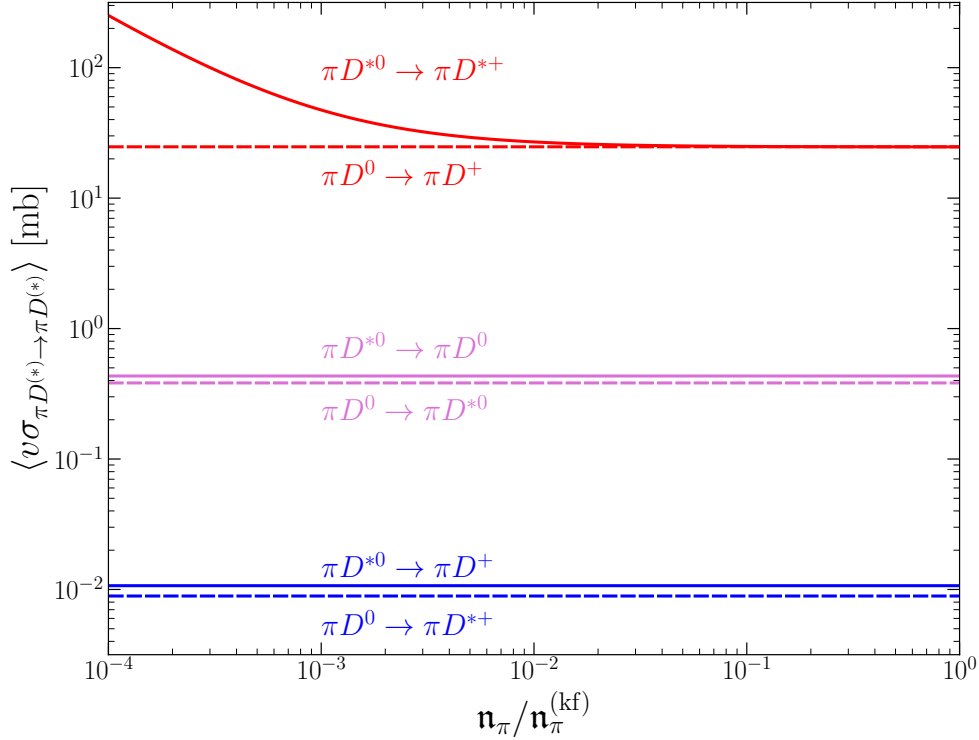


FIG. 11. Reaction rates $\langle v\sigma_{\pi D^{(*)} \rightarrow \pi D^{(*)}} \rangle$ for the scattering of an incoming neutral charm meson D^0 or D^{*0} and a pion in the hadron gas after kinetic freezeout as functions of the pion number density n_π : $\pi D^0 \rightarrow \pi D^+$, $\pi D^0 \rightarrow \pi D^{*0}$, $\pi D^0 \rightarrow \pi D^{*+}$ (dashed curves: higher red, intermediate purple, and lower blue), $\pi D^{*0} \rightarrow \pi D^{*+}$, $\pi D^{*0} \rightarrow \pi D^0$, $\pi D^{*0} \rightarrow \pi D^+$ (solid curves: higher red, intermediate purple, and lower blue). The increase in the reaction rate for $\pi D^{*0} \rightarrow \pi D^{*+}$ as $n_\pi \rightarrow 0$ comes from a D -meson t -channel singularity.

of n_π . There can also be dependence on T or n_π through the mass shifts in $\Gamma_{D^{*a} \rightarrow D^b \pi}$ and through the factors of $1/\Gamma_c$.

After kinetic freezeout, the most dramatic dependences on n_π can be made explicit by inserting the expressions for the thermal widths of D^+ and D^0 in Eqs. (57). The resulting expression for the reaction rate for $\pi D^{*0} \rightarrow \pi D^{*+}$ (or $\pi D^{*+} \rightarrow \pi D^{*0}$) is

$$\langle v\sigma_{\pi D^{*0} \rightarrow \pi D^{*+}} \rangle = (0.991 + 0.306 g_\pi^4) \frac{m_\pi^2}{f_\pi^4} + \frac{1}{3n_\pi} \frac{\Gamma_{D^{*0} \rightarrow D^0 \pi} \Gamma_{D^{*+} \rightarrow D^0 \pi}}{\Gamma_{D^{*0} \rightarrow D^0 \pi} + \Gamma_{D^{*+} \rightarrow D^0 \pi}}. \quad (85)$$

At kinetic freezeout, the t -channel singularity term is smaller than the nonsingular term by the factor 0.0003. However the multiplicative factor of $1/n_\pi$ makes the t -channel singularity term increase dramatically as the hadron gas expands. It becomes equal to the nonsingular term when n_π decreases by the factor 0.0009. Since the volume $V(\tau)$ of the hadron gas increases roughly as τ^3 , this corresponds to an increase in its linear dimensions by about a factor of 10.

Many of the $\pi D^{(*)} \rightarrow \pi D^{(*)}$ scattering reactions change the flavor or spin of the charm meson. The reaction rates in the hadron gas after kinetic freezeout at $T_{\text{kf}} = 115$ MeV for incoming neutral charm mesons D^0 or D^{*0} are shown as functions of the pion number

density \mathbf{n}_π in Fig. 11. For each of these reactions, there is another one with an incoming charged charm meson D^+ or D^{*+} that has the same reaction rate. The reaction rate for $\pi D^0 \rightarrow \pi D^+$ is given in Eq. (69b). The reaction rates for $\pi D^0 \rightarrow \pi D^{*0}$ and $\pi D^0 \rightarrow \pi D^{*+}$ are given in Eqs. (75a) and (75b). The reaction rates for $\pi D^{*0} \rightarrow \pi D^0$ and $\pi D^{*0} \rightarrow \pi D^+$ are given in Eqs. (76a) and (76b). The largest reaction rates in Fig. 11 are for reactions that change the charm-meson flavor only. The reaction rate for $\pi D^0 \rightarrow \pi D^+$ has a D^{*+} resonance contribution that makes it increase as \mathbf{n}_π decreases. However the D^{*+} resonance contribution is about 3 orders of magnitude smaller than the nonresonant term, so the decrease is not visible in Fig. 11. The reaction rate for $\pi D^{*0} \rightarrow \pi D^{*+}$ has a D^0 t -channel singularity contribution that makes it diverge as $\mathbf{n}_\pi \rightarrow 0$. The other reaction rates in Fig. 11 are constant functions of \mathbf{n}_π . The rates in Fig. 11 for reactions that change the charm-meson spin are suppressed by more than 1.5 orders of magnitude. The rates for reactions that change both the flavor and spin of the charm meson are suppressed by more than 3 orders of magnitude.

VI. EVOLUTION OF CHARM-MESON RATIOS

In this section, we calculate the evolution of the charm-meson number densities in the expanding hadron gas from a heavy-ion collision after kinetic freezeout.

A. Rate equations

The evolution of the number density $\mathbf{n}_{D^{(*)}}(\tau)$ of a charm meson in the expanding hadron gas with the proper time τ can be described by a first order differential equation. The number density decreases because of the increasing volume $V(\tau)$, but it can also be changed by reactions. The time derivative of $\mathbf{n}_{D^{(*)}}$ has positive contributions from reactions with $D^{(*)}$ in the final state and negative contributions from reactions with $D^{(*)}$ in the initial state. Near kinetic freezeout, the most important reactions involve pions, because pions are by far the most abundant hadrons in the hadron gas.

After kinetic freezeout, most interactions have a negligible effect on the number density $\mathbf{n}_{D^{(*)}}(\tau)$ of a charm meson. The charm-meson number density decreases in proportion to $1/V(\tau)$, like the pion number density $\mathbf{n}_\pi(\tau)$ in Eq. (19). The effect of the increasing volume can be removed from the differential equation by considering the rate equation for the ratio of number densities $\mathbf{n}_{D^{(*)}}/\mathbf{n}_\pi$. The remaining terms in the rate equation come from reactions that change the spin or flavor of the charm meson. The reaction rate is multiplied by a factor of the number density for every particle in the initial state. The reaction rate is determined by the temperature, which is fixed at the kinetic freezeout temperature T_{kf} , the charm-meson number density $\mathbf{n}_{D^{(*)}}$, and the pion number density $\mathbf{n}_\pi(\tau)$, which decreases as $1/V(\tau)$. Some reaction rates in the expanding hadron gas are sensitive to the thermal mass shifts and the thermal widths of the hadrons. The greatest sensitivities to the thermal mass shifts for charm mesons and pions are in reactions whose rates are proportional to a power of $M_{D^*} - M_D - m_\pi$, such as $D^* \rightarrow D\pi$ decay rates. The greatest sensitivity to the thermal width Γ_a of a pseudoscalar charm meson D^a comes from D -meson t -channel singularities, which can produce contributions to reaction rates proportional to $1/\Gamma_a$ in the limit $\Gamma_a \rightarrow 0$.

The most relevant reactions for charm mesons in the expanding hadron gas include the

decays $D^* \rightarrow D\pi$ and $D^* \rightarrow D\gamma$, the scattering reactions $\pi D \rightarrow \pi D$, $\pi D \rightarrow D\gamma$, and $\pi D^* \rightarrow \pi D^*$ that change the charm-meson flavor, and the scattering reactions $\pi D \rightarrow \pi D^*$ and $\pi D^* \rightarrow \pi D$ that change the charm-meson spin. The rate equations for the number densities of the pseudoscalar charm mesons D^a and the vector charm mesons D^{*a} are

$$\begin{aligned} \mathbf{n}_\pi \frac{d}{d\tau} \left(\frac{\mathbf{n}_{D^a}}{\mathbf{n}_\pi} \right) &= [1 + \mathfrak{f}_\pi(m_\pi)] \sum_b \Gamma_{D^{*b} \rightarrow D^a \pi} \mathbf{n}_{D^{*b}} + \Gamma_{*a, \gamma} \mathbf{n}_{D^{*a}} \\ &+ 3 \sum_{b \neq a} [\langle v\sigma_{\pi D^b \rightarrow \pi D^a} \rangle (\mathbf{n}_{D^b} - \mathbf{n}_{D^a}) + \langle v\sigma_{\pi D^b \rightarrow D^a \gamma} \rangle \mathbf{n}_{D^b} - \langle v\sigma_{\pi D^a \rightarrow D^b \gamma} \rangle \mathbf{n}_{D^a}] \mathbf{n}_\pi \\ &+ 3 \sum_b [\langle v\sigma_{\pi D^{*b} \rightarrow \pi D^a} \rangle \mathbf{n}_{D^{*b}} - \langle v\sigma_{\pi D^a \rightarrow \pi D^{*b}} \rangle \mathbf{n}_{D^a}] \mathbf{n}_\pi + \dots, \end{aligned} \quad (86a)$$

$$\begin{aligned} \mathbf{n}_\pi \frac{d}{d\tau} \left(\frac{\mathbf{n}_{D^{*a}}}{\mathbf{n}_\pi} \right) &= - \left([1 + \mathfrak{f}_\pi(m_\pi)] \sum_b \Gamma_{D^{*a} \rightarrow D^b \pi} + \Gamma_{*a, \gamma} \right) \mathbf{n}_{D^{*a}} \\ &+ 3 \sum_{b \neq a} \langle v\sigma_{\pi D^{*b} \rightarrow \pi D^{*a}} \rangle (\mathbf{n}_{D^{*b}} - \mathbf{n}_{D^{*a}}) \mathbf{n}_\pi \\ &+ 3 \sum_b [\langle v\sigma_{\pi D^b \rightarrow \pi D^{*a}} \rangle \mathbf{n}_{D^b} - \langle v\sigma_{\pi D^{*a} \rightarrow \pi D^b} \rangle \mathbf{n}_{D^a}] \mathbf{n}_\pi + \dots \end{aligned} \quad (86b)$$

The partial decay rates $\Gamma_{D^{*a} \rightarrow D^b \pi}$ and $\Gamma_{*a, \gamma}$ are given in Eqs. (56) and (6). The reaction rates $\langle v\sigma_{\pi D^a \rightarrow \pi D^b} \rangle$ and $\langle v\sigma_{\pi D^a \rightarrow D^b \gamma} \rangle$, which have D^* resonance contributions, are given in Eqs. (69) and (70). The reaction rates $\langle v\sigma_{\pi D^a \rightarrow \pi D^{*b}} \rangle$ and $\langle v\sigma_{\pi D^{*a} \rightarrow \pi D^b} \rangle$ are given in Eqs. (75) and (76). The reaction rates $\langle v\sigma_{\pi D^{*a} \rightarrow \pi D^{*b}} \rangle$, which have D -meson t -channel singularities, are given in Eqs. (84). The rate equations in Eqs. (86) are consistent with the conservation of charm-quark number, which implies that the sum of the ratios of the number densities for all four charm mesons remains constant:

$$\mathbf{n}_\pi \frac{d}{d\tau} \left(\frac{\mathbf{n}_{D^0} + \mathbf{n}_{D^+} + \mathbf{n}_{D^{*0}} + \mathbf{n}_{D^{*+}}}{\mathbf{n}_\pi} \right) = 0. \quad (87)$$

Given initial conditions on the ratios $\mathbf{n}_{D^{(*)}}(\tau)/\mathbf{n}_\pi(\tau)$ of charm-meson and pion number densities, the rate equations in Eqs. (86) can be integrated to determine the ratios at larger τ . As our initial conditions on the ratio at kinetic freezeout, we take the ratio of the multiplicity of the charm meson before D^* decays and the pion multiplicity:

$$\frac{\mathbf{n}_{D^a}(\tau_{\text{kf}})}{\mathbf{n}_\pi(\tau_{\text{kf}})} = \frac{(dN_{D^a}/dy)_0}{dN_\pi/dy}, \quad (88a)$$

$$\frac{\mathbf{n}_{D^{*a}}(\tau_{\text{kf}})}{\mathbf{n}_\pi(\tau_{\text{kf}})} = \frac{(dN_{D^{*a}}/dy)_0}{dN_\pi/dy}. \quad (88b)$$

In the case of Pb-Pb collisions in the centrality range 0-10% at $\sqrt{s_{NN}} = 5.02$ TeV, the multiplicity dN_π/dy for a single pion flavor measured by the ALICE collaboration is given in Eq. (22) [25]. The multiplicities $(dN_{D^{*a}}/dy)_0$ and $(dN_{D^a}/dy)_0$ for charm mesons before D^* decays inferred from SHM predictions are given in Eqs. (26) and (27). The resulting initial values of the ratios of charm-meson and pion number densities at kinetic freezeout for D^0 , D^+ , D^{*0} , and D^{*+} are 0.00278, 0.00264, 0.00334, and 0.00328, respectively.

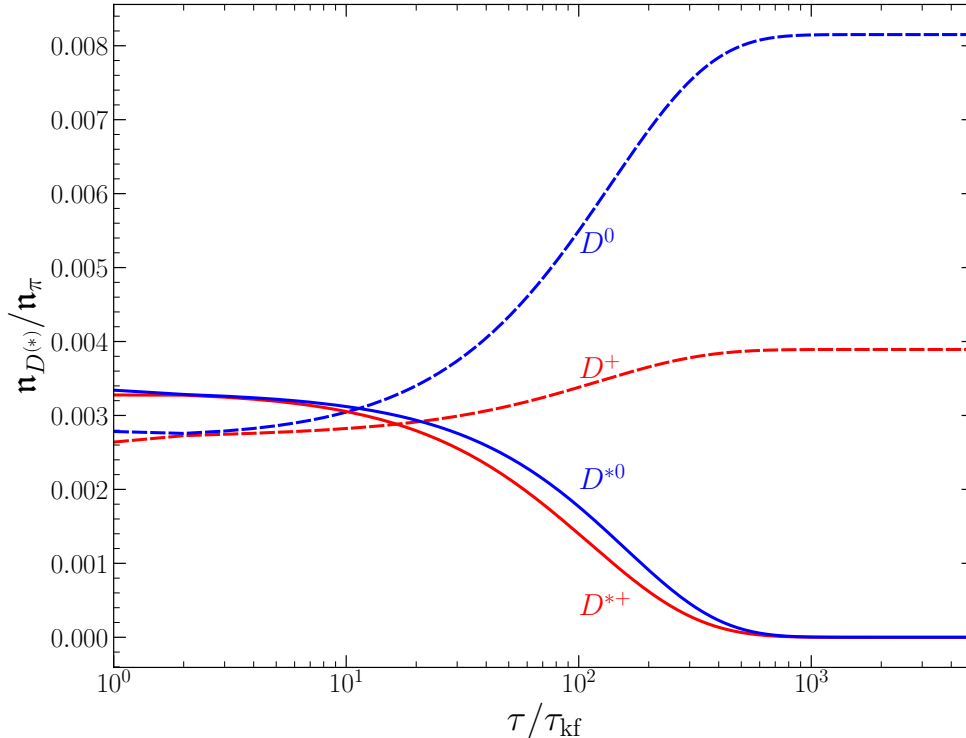


FIG. 12. Proper-time evolution of the ratios of number densities of charm meson and pions from solving the rate equations in Eqs. (86): n_{D^0}/n_{π} , n_{D^+}/n_{π} (dashed curves: higher blue, lower red), $n_{D^{*0}}/n_{\pi}$, $n_{D^{*+}}/n_{\pi}$ (solid curves: higher blue, lower red).

The solutions to the rate equations in Eqs. (86) with the initial conditions in Eqs. (88) are shown in Fig. 12. The ratios $n_{D^{*0}}/n_{\pi}$ and $n_{D^{*+}}/n_{\pi}$ decrease exponentially to 0 on time scales comparable to the D^* lifetimes. The ratio N_{D^0}/N_{D^+} of the numbers of D^0 and D^+ is predicted to increase from 1.053 at kinetic freezeout to about 2.092 at the detector. The naive prediction for the effects of D^* decays on the numbers N_{D^0} and N_{D^+} at the detector can be obtained by inserting the initial conditions at kinetic freezeout into Eqs. (9). The naive prediction for the ratio N_{D^0}/N_{D^+} at the detector is 2.255. This is about 10% larger than the ratio from solving the rate equations. Thus the rate equations in Eqs. (86) must include reactions other than D^* decays whose effects are not negligible after kinetic freezeout.

B. Asymptotic Evolution

As τ increases, the pion number density $n_{\pi}(\tau)$ decreases to 0 as $1/V(\tau)$. As n_{π} approaches 0, most of the reaction rates in Eqs. (86) approach the finite constant reaction rates in the vacuum. The exceptions are $\langle v\sigma_{\pi D^{*0} \rightarrow \pi D^{*+}} \rangle$ and $\langle v\sigma_{\pi D^{*+} \rightarrow \pi D^{*0}} \rangle$, which are given in Eqs. (84b) and (84c). They have contributions with a factor of $1/\Gamma_0$ from a D -meson t -channel singularity. Since Γ_0 , which is given in Eq. (57b), decreases to 0 in proportion to n_{π} as $n_{\pi} \rightarrow 0$, these reaction rates increase as $1/n_{\pi}$. The limiting behaviors of the reaction

rates $\langle v\sigma_{\pi D^{*b} \rightarrow \pi D^{*a}} \rangle$ as $\mathbf{n}_\pi \rightarrow 0$ in Eqs. (84) are

$$\langle v\sigma_{\pi D^{*0} \rightarrow \pi D^{*0}} \rangle \longrightarrow \frac{1}{3\mathbf{n}_\pi} \frac{(B_{00}\Gamma_{*0})^2}{B_{00}\Gamma_{*0} + B_{+0}\Gamma_{*+}}, \quad (89a)$$

$$\langle v\sigma_{\pi D^{*0} \rightarrow \pi D^{*+}} \rangle \longrightarrow \frac{1}{3\mathbf{n}_\pi} \frac{(B_{00}\Gamma_{*0})(B_{+0}\Gamma_{*+})}{B_{00}\Gamma_{*0} + B_{+0}\Gamma_{*+}}, \quad (89b)$$

$$\langle v\sigma_{\pi D^{*+} \rightarrow \pi D^{*0}} \rangle \longrightarrow \frac{1}{3\mathbf{n}_\pi} \frac{(B_{00}\Gamma_{*0})(B_{+0}\Gamma_{*+})}{B_{00}\Gamma_{*0} + B_{+0}\Gamma_{*+}}, \quad (89c)$$

$$\langle v\sigma_{\pi D^{*+} \rightarrow \pi D^{*+}} \rangle \longrightarrow \frac{1}{3\mathbf{n}_\pi} \left(\frac{(B_{+0}\Gamma_{*+})^2}{B_{00}\Gamma_{*0} + B_{+0}\Gamma_{*+}} + B_{++}\Gamma_{*+} \right), \quad (89d)$$

where Γ_{*a} is the decay rate for D^{*a} in the vacuum given in Eqs. (5) and B_{ab} is the branching fraction for $D^{*a} \rightarrow D^b\pi$ given in Eqs. (4). The factors of $1/\mathbf{n}_\pi$ in these asymptotic reaction rates can cancel explicit factors of \mathbf{n}_π in the rate equations.

At large times τ , the only terms in the rate equation that survive are 1-body terms with a single factor of a number density \mathbf{n}_D or \mathbf{n}_{D^*} . There are 1-body terms from the decays $D^* \rightarrow D\pi$ and $D^* \rightarrow D\gamma$. The t -channel singularities produce additional 1-body terms. If the 1-body terms from D -meson t -channel singularities are taken into account, the asymptotic rate equations become

$$\mathbf{n}_\pi \frac{d}{d\tau} \left(\frac{\mathbf{n}_{D^+}}{\mathbf{n}_\pi} \right) \longrightarrow (1 - B_{+0})\Gamma_{*+}\mathbf{n}_{D^{*+}}, \quad (90a)$$

$$\mathbf{n}_\pi \frac{d}{d\tau} \left(\frac{\mathbf{n}_{D^0}}{\mathbf{n}_\pi} \right) \longrightarrow \Gamma_{*0}\mathbf{n}_{D^{*0}} + B_{+0}\Gamma_{*+}\mathbf{n}_{D^{*+}}, \quad (90b)$$

$$\mathbf{n}_\pi \frac{d}{d\tau} \left(\frac{\mathbf{n}_{D^{*+}}}{\mathbf{n}_\pi} \right) \longrightarrow -(\Gamma_{*+} + \gamma)\mathbf{n}_{D^{*+}} + \gamma\mathbf{n}_{D^{*0}}, \quad (90c)$$

$$\mathbf{n}_\pi \frac{d}{d\tau} \left(\frac{\mathbf{n}_{D^{*0}}}{\mathbf{n}_\pi} \right) \longrightarrow -(\Gamma_{*0} + \gamma)\mathbf{n}_{D^{*0}} + \gamma\mathbf{n}_{D^{*+}}, \quad (90d)$$

where the rate γ is

$$\gamma = \frac{1}{1/(B_{00}\Gamma_{*0}) + 1/(B_{+0}\Gamma_{*+})} = 21.9 \text{ keV}. \quad (91)$$

The terms in Eqs. (90) with the factor γ come from D -meson t -channel singularities.

The asymptotic rate equations in Eqs. (90) can be solved analytically. If the numbers of D^0 , D^+ , D^{*0} , and D^{*+} at kinetic freezeout are $(N_{D^0})_0$, $(N_{D^+})_0$, $(N_{D^{*0}})_0$, and $(N_{D^{*+}})_0$, the predicted asymptotic numbers of D^0 and D^+ are

$$N_0 = (N_0)_0 + (N_{*0})_0 + B_{+0}(N_{*+})_0 - \frac{(1 - B_{+0})\gamma}{\Gamma_{*+}\Gamma_{*0} + (\Gamma_{*+} + \Gamma_{*0})\gamma} [\Gamma_{*+}(N_{*0})_0 - \Gamma_{*0}(N_{*+})_0], \quad (92a)$$

$$N_+ = (N_+)_0 + (1 - B_{+0})(N_{*+})_0 + \frac{(1 - B_{+0})\gamma}{\Gamma_{*+}\Gamma_{*0} + (\Gamma_{*+} + \Gamma_{*0})\gamma} [\Gamma_{*+}(N_{*0})_0 - \Gamma_{*0}(N_{*+})_0], \quad (92b)$$

where γ is given in Eq. (91). The coefficients of $(N_{*0})_0$ and $(N_{*+})_0$ in Eqs. (92) depend only on B_{+0} , B_{00} , and the ratio Γ_{*0}/Γ_{*+} . The prediction for the difference between the numbers

of D^0 and D^+ are

$$N_0 - N_+ = 2B_{+0}(N_{*+})_0 + (N_0 - N_+)_0 + (N_{*0} - N_{*+})_0 - \frac{2(1 - B_{+0})\gamma}{\Gamma_{*+}\Gamma_{*0} + (\Gamma_{*+} + \Gamma_{*0})\gamma} [\Gamma_{*+}(N_{*0})_0 - \Gamma_{*0}(N_{*+})_0]. \quad (93)$$

If we impose the isospin-symmetry approximations $(N_0)_0 \approx (N_+)_0$ and $(N_{*0})_0 \approx (N_{*+})_0$, the difference reduces to

$$N_0 - N_+ \approx 2 \left(B_{+0} - \frac{(1 - B_{+0})(\Gamma_{*+} - \Gamma_{*0})\gamma}{\Gamma_{*+}\Gamma_{*0} + (\Gamma_{*+} + \Gamma_{*0})\gamma} \right) (N_{*+})_0. \quad (94)$$

The two terms in the parantheses come from D^* decays and the D -meson t -channel singularity, respectively. The effect of D -meson t -channel singularities is to reduce the coefficient of $(N_{*+})_0$ from 1.35 ± 0.01 , which includes the effects of D^* decays only, to 1.30 ± 0.01 . The change in the coefficient is small but statistically significant.

We use our initial conditions on the ratios of the charm-meson/pion number densities at kinetic freezeout to illustrate the effect of t -channel singularities on the ratio N_0/N_+ of the observed numbers of D^0 and D^+ . The ratio before D^* decays is $(N_{D^0})_0/(N_{D^+})_0 = 1.053$. The predicted numbers of D^0 and D^+ at the detector are given in Eqs. (92). Their ratio is predicted to increase to 2.178 ± 0.016 at the detector, where the error bar is from B_{+0} , B_{00} , Γ_{*0} , and Γ_{*+} only. The naive ratio N_{D^0}/N_{D^+} ignoring t -channel singularities, which is obtained using Eqs. (9), is 2.255 ± 0.014 . The difference between the predicted ratio taking into account t -channel singularities and the naive prediction is -0.077 ± 0.006 , which differs from 0 by about 13 standard deviations.

VII. CONCLUSION

The reactions $\pi D^* \rightarrow \pi D^*$ have t -channel singularities in 6 of the 10 scattering channels. These reactions can proceed at tree level through the decay $D^* \rightarrow \pi D$ followed by the inverse decay $\pi D \rightarrow D^*$. The t -channel singularity appears because the intermediate D can be on shell. The tree-level cross section diverges inside a narrow interval of the center-of-mass energy near the threshold, which is given by Eq. (1) if the incoming and outgoing π and D have the same flavor. If the singularity is regularized by inserting the width Γ of the D into its propagator, the cross section has a term with a factor of the D lifetime $1/\Gamma$. The resulting enormous cross section is unphysical, because the lifetimes of the incoming and outgoing D^* are many orders of magnitude smaller than the D lifetime. A more physical regularization of the t -channel singularity in the reaction rate for $\pi D^* \rightarrow \pi D^*$ could perhaps be obtained by a resummation of loop diagrams. There are n -loop diagrams with $n + 1$ D propagators, n D^* propagators, and n pion propagators in which all $2n + 1$ charm-meson propagators are nearly on shell. A resummation of these diagrams to all orders could produce a regularization of the t -channel singularity that is determined by the D^* width.

As pointed out by Grzadkowski, Igllicki, and Mrówczyński in Ref. [1], the thermal widths of particles in a medium provide a physical regularization of t -channel singularities. In a hadronic medium, the t -channel singularity in the reaction rate for $\pi D^* \rightarrow \pi D^*$ is regularized by the thermal width of D . A physical example of such a hadronic medium is the hadron gas produced by a central relativistic heavy-ion collision. The effects of the hadron

gas are particularly simple near and after kinetic freezeout, because it can be accurately approximated by a pion gas. The thermal widths of the charm mesons come primarily from coherent pion forward scattering. At leading order in the pion interactions, the thermal widths Γ_+ of D^+ and Γ_0 of D^0 are given by Eqs. (57). Before kinetic freezeout, the D widths are determined by the decreasing temperature T . After kinetic freezeout, the D widths are determined by the kinetic freezeout temperature and the decreasing pion number density \mathbf{n}_π .

In a hadronic medium, the t -channel singularities in the reaction rates for $\pi D^* \rightarrow \pi D^*$ produce terms in the average reaction rates $\langle v\sigma_{\pi D^* \rightarrow \pi D^*} \rangle$ inversely proportional to the thermal widths Γ_+ and Γ_0 . These terms come from πD^* scattering in regions near the threshold, and they are sensitive to differences $\Delta - m_\pi$ between $D^* - D$ mass differences in the medium and pion masses in the medium. There are also nonsingular contributions from πD^* scattering that are determined primarily by the temperature T and are insensitive to the values of $\Delta - m_\pi$. We found a simple prescription for the nonsingular reaction rates that allowed the total reaction rate to be approximated by the sum of the nonsingular term and the t -channel singularity terms. Our prescription for the nonsingular reaction rate is simply the rate in the limit $\Delta \rightarrow m_\pi$. The resulting expressions for the reaction rates $\langle v\sigma_{\pi D^{*a} \rightarrow \pi D^{*b}} \rangle$ in the pion gas after kinetic freezeout are given in Eqs. (84). After kinetic freezeout, the most dramatic dependence of reaction rates for $\pi D^* \rightarrow \pi D^*$ on \mathbf{n}_π comes from a multiplicative factor of $1/\mathbf{n}_\pi$. This dependence for $\langle v\sigma_{\pi D^{*0} \rightarrow \pi D^{*+}} \rangle$ is made explicit in Eq. (85).

In rate equations for the evolution of number densities, a reaction rate is multiplied by the number density of each of the incoming particles. In the hadron gas after kinetic freezeout, all the number densities are decreasing in inverse proportion to the expanding volume $V(\tau)$. Thus n -body reactions, which have $n \geq 2$ incoming particles, are suppressed compared to decays, which are 1-body reactions, by the additional factors of the number densities. A 2-body reaction whose rate is proportional to an inverse power of a number density provides an exception, because its effects in the rate equation can be comparable to 1-body terms. In particular, the effects of the reactions $\pi D^* \rightarrow \pi D^*$ can be comparable to 1-body terms because of the multiplicative factor of $1/\mathbf{n}_\pi$ in the t -channel singularity term. Rate equations for the number density ratios $\mathbf{n}_{D^a}/\mathbf{n}_\pi$ and $\mathbf{n}_{D^{*a}}/\mathbf{n}_\pi$ are given in Eqs. (86). The numerical solutions of these rate equations after kinetic freezeout for specific initials conditions motivated by the Statistical Hadronization Model are illustrated in Fig. 12. There is a small but significant difference between the asymptotic charm-meson ratios and the naive predictions from Eqs. (9), which take into account only the decays of D^{*0} and D^{*+} .

The asymptotic forms of the rate equations in the limit $\mathbf{n}_\pi \rightarrow 0$ are given in Eqs. (90). The only rates that remain in that limit are 1-body terms, but those terms come not only from D^* decays but also from the t -channel singularities in $\pi D^* \rightarrow \pi D^*$ reactions. The rates are completely determined by D^* decay rates and D^* branching fractions in the vacuum. From the analytic solutions of the asymptotic rate equations, we deduced the simple approximations in Eqs. (92) for the asymptotic numbers of D^0 and D^+ given the numbers of the D^0 , D^+ , D^{*0} , and D^{*+} at kinetic freezeout. The new terms from t -channel singularities are those with a factor of the rate γ . The predicted deviations of charm-meson ratios from the naive predictions from Eqs. (9) are small but much larger than the statistical errors from the D^* decay rates and branching fractions. The analytic predictions from Eqs. (92) give good approximations to numerical solutions of the more accurate rate equations in Eqs. (86).

There are other charm-meson reactions with t -channel singularities including $\pi D^* \rightarrow \pi\pi D$ and $\pi\pi D \rightarrow \pi D^*$. The reaction $\pi D^* \rightarrow \pi\pi D$ has a pion t -channel singularity from the

decay $D^* \rightarrow D\pi$ followed by the scattering $\pi\pi \rightarrow \pi\pi$. In a hadronic medium, the t -channel singularity is regularized by the thermal width Γ_π of the pion. In a pion gas, the leading term in Γ_π is proportional to \mathbf{n}_π . Our preliminary result for the t -channel singularity contribution to the reaction rate for $\pi D^* \rightarrow \pi\pi D$ can be reduced to $\Gamma_{D^* \rightarrow D\pi}/\mathbf{n}_\pi$, which is comparable to the t -channel singularity term in the reaction rate for $\pi D^{*0} \rightarrow \pi D^{*+}$ in Eq. (85). This suggests that the contributions from pion t -channel singularities may be comparable to those from D -meson t -channel singularities.

There have been previous studies of the effects of a thermal hadronic medium on charm mesons [31–34]. In these studies, isospin splittings have been ignored and therefore the possibility of t -channel singularities has not been considered. It might be worthwhile to look for other aspects of the thermal physics of charm mesons in which the effects of t -channel singularities are significant. One such aspect is the production of the exotic heavy hadrons $X(3872)$ and $T_{cc}^+(3875)$. Their tiny binding energies relative to a charm-meson-pair threshold imply that they are loosely bound charm-meson molecules. In previous studies of the production of charm-meson molecules, it has been assumed that they are produced before kinetic freezeout [16, 35–40]. It is possible that t -channel singularities could have a significant effect on their production after kinetic freezeout.

The problem of t -channel singularities is an unavoidable aspect of reactions involving unstable particles. Unstable particles are ubiquitous in hadronic physics. In the Standard Model of particle physics, the weak bosons and the Higgs are unstable particles. Most models of physics beyond the Standard Model have unstable particles. We have identified a simple aspect of charm-meson physics in which the effects of t -channel singularities are significant. This provides encouragement to look for other effects of t -channel singularities in hadronic, nuclear, and particle physics.

ACKNOWLEDGMENTS

KI would like to thank Ulrich Heinz for many helpful discussions during the early stages of this project. This work was supported in part by the U.S. Department of Energy under grant DE-SC0011726, by the Ministry of Science, Innovation and Universities of Spain under grant BES-2017-079860, by the National Natural Science Foundation of China (NSFC) under grant 11905112, by the Natural Science Foundation of Shandong Province of China under grant ZR2019QA012, by the Alexander von Humboldt Foundation, and by NSFC and the Deutsche Forschungsgemeinschaft (DFG) through the Sino-German Collaborative Research Center TRR110 (NSFC grant 12070131001, DFG Project-ID 196253076-TRR110).

Appendix A: Feynman rules for HH χ EFT

In χ EFT, the propagator for a pion with momentum p and isospin indices i, j is

$$\boxed{\frac{i \delta^{ij}}{p^2 - m_\pi^2 + i\epsilon}}. \quad (\text{A1})$$

At LO in χ EFT, the only interaction parameter for pions is the pion decay constant f_π . The four-pion vertex is

$$\pi^i(p)\pi^j(q) \rightarrow \pi^m(p')\pi^n(q') : \quad \boxed{\frac{2i}{f_\pi^2} \left[s \delta^{ij} \delta^{mn} + t \delta^{im} \delta^{jn} + u \delta^{in} \delta^{jm} - \frac{3m_\pi^2 + Q^2}{3} (\delta^{ij} \delta^{mn} + \delta^{im} \delta^{jn} + \delta^{in} \delta^{jm}) \right]}, \quad (\text{A2})$$

where the Mandelstam variables are $s = (p + q)^2$, $t = (p - p')^2$, and $u = (p - q')^2$ and $Q^2 = p^2 + q^2 + p'^2 + q'^2 - 4m_\pi^2$.

The interactions of charm mesons with pions can be described using heavy-hadron chiral effective field theory (HH χ EFT). In HH χ EFT, the 4-momentum of a charm meson is expressed as the sum of Mv , with v a velocity 4-vector that satisfies $v^2 = 1$, and a residual 4-momentum p . The propagator for a pseudoscalar charm meson D with momentum $Mv + p$ and isospin indices a, b is

$$\boxed{\frac{i \delta_{ab}}{2(v \cdot p + i\epsilon)}}. \quad (\text{A3})$$

In amplitudes that are sensitive to isospin splittings, $v \cdot p$ in the propagator for D^a should be replaced by $v \cdot p - (M_a - M)$. If D^a can be on its mass shell, the term $+i\epsilon$ in the denominator should be replaced by $+i\Gamma_a/2$, where Γ_a is the width of D^a . The propagator for a vector charm meson D^* with momentum $Mv + p$ and isospin indices a, b is

$$\boxed{\frac{i \delta_{ab} (-g_{\mu\nu} + v_\mu v_\nu)}{2(v \cdot p - \Delta + i\epsilon)}}, \quad (\text{A4})$$

where $\Delta = M_* - M$ is the mass difference between the vector and pseudoscalar meson. The mass shell for $D^{(*)}$ is $v \cdot p = \Delta$. In amplitudes that are sensitive to isospin splittings, $v \cdot p - \Delta$ in the propagator for D^{*a} should be replaced by $v \cdot p - (M_{*a} - M)$. If D^{*a} can be on its mass shell, the term $+i\epsilon$ in the denominator should be replaced by $+i\Gamma_{*a}/2$, where Γ_{*a} is the width of D^{*a} .

The interactions between charm meson and pions in HH χ EFT at LO are determined by the pion decay constant f_π and a dimensionless coupling constant g_π . The vertices for $D^{(*)} \pi \rightarrow D^{(*)} \pi$ are

$$D^a \pi^i(q) \longrightarrow D^b \pi^j(q') : \quad \boxed{+\frac{i}{2f_\pi^2} v \cdot (q + q') [\sigma^i, \sigma^j]_{ab}}, \quad (\text{A5a})$$

$$D_\mu^{*a} \pi^i(q) \longrightarrow D_\nu^{*b} \pi^j(q') : \quad \boxed{-\frac{i}{2f_\pi^2} g^{\mu\nu} v \cdot (q + q') [\sigma^i, \sigma^j]_{ab}}. \quad (\text{A5b})$$

The vertices for $D^{(*)} \rightarrow D^{(*)} \pi(q)$ are

$$D_\mu^{*a} \longrightarrow D^b \pi^i(q) : \quad \boxed{+i \frac{\sqrt{2} g_\pi}{f_\pi} \sigma_{ab}^i q^\mu}, \quad (\text{A6a})$$

$$D^a \longrightarrow D_\mu^{*b} \pi^i(q) : \quad \boxed{-i \frac{\sqrt{2} g_\pi}{f_\pi} \sigma_{ab}^i q^\mu}, \quad (\text{A6b})$$

$$D_\mu^{*a} \longrightarrow D_\nu^{*b} \pi^i(q) : \quad \boxed{+i \frac{\sqrt{2} g_\pi}{f_\pi} \sigma_{ab}^i \epsilon^{\mu\nu\alpha\beta} v_\alpha q_\beta}. \quad (\text{A6c})$$

The vertices for $D^{(*)}\pi(q) \rightarrow D^{(*)}$ are obtained by replacing q by $-q$. Our convention for the Levi-Civita tensor in Eq. (A6c) is $\epsilon_{0123} = +1$.

Appendix B: Integrals over the Momentum of a Thermal Pion

In this Appendix, we evaluate the integrals over the pion momentum that appear in the on-shell charm-meson self energies in HH χ EFT at LO.

1. $i\epsilon$ Prescriptions

The on-shell self energies for the charm mesons D^a and D^{*a} are given in Eqs. (41) and (50). The thermal average that appears in these self energies is

$$\mathcal{F}_{cd} = \left\langle \frac{q^2}{\omega_{cdq}(q^2 - q_{cd}^2 + i\epsilon)} \right\rangle, \quad (\text{B1})$$

where $\omega_{cdq} = \sqrt{m_{\pi cd}^2 + q^2}$, $q_{cd}^2 = \Delta_{cd}^2 - m_{\pi cd}^2$, Δ_{cd} is the D^{*c} - D^d mass splitting, and $m_{\pi cd}$ is the mass of the pion produced by the transition $D^{*c} \rightarrow D^d \pi^i$. The angular brackets represent the average over the Bose-Einstein momentum distribution of the pion, which is defined in Eq. (21) as the ratio of momentum integrals.

The numerator of the thermal average \mathcal{F}_{cd} in Eq. (B1) can be expressed as an integral over a single momentum variable of the form

$$\mathcal{F}(\sigma) = \lim_{\epsilon \rightarrow 0^+} \int_0^\infty dq \frac{F(q^2)}{q^2 - \sigma + i\epsilon}, \quad (\text{B2})$$

where $F(q^2)$ is a smooth, real-valued function that decreases as q^4 as $q \rightarrow 0$ and decreases exponentially to 0 as $q \rightarrow \infty$. The real parameter σ , which can be positive or negative, is small compared to the scale of q^2 set by $F(q^2)$. We would like to expand $\mathcal{F}(\sigma)$ in powers of σ .

The function $\mathcal{F}(\sigma)$ can be expressed as the sum of a principal-value integral and the integral of a delta function:

$$\begin{aligned} \mathcal{F}(\sigma) &= \int_0^\infty dq F(q^2) \left(\mathcal{P} \frac{1}{q^2 - \sigma} - i\pi \delta(q^2 - \sigma) \right) \\ &= \int_0^\infty dq \frac{F(q^2) - F(\sigma)}{q^2 - \sigma} - i \frac{\pi}{2\sqrt{\sigma}} F(\sigma) \theta(\sigma). \end{aligned} \quad (\text{B3})$$

We have used an identity to express the principal-value integral in terms of an ordinary integral. The Taylor expansion of the real part of $\mathcal{F}(\sigma)$ can be obtained by expanding the integrand in the second line of Eq. (B3) as a Taylor expansion in σ :

$$\begin{aligned} \text{Re}[\mathcal{F}(\sigma)] &= \int_0^\infty dq \frac{F(q^2) - F(0)}{q^2} + \sigma \int_0^\infty dq \frac{F(q^2) - F(0) - F'(0)q^2}{q^4} \\ &\quad + \sigma^2 \int_0^\infty dq \frac{F(q^2) - F(0) - F'(0)q^2 - \frac{1}{2}F''(0)q^4}{q^6} + \dots \end{aligned} \quad (\text{B4})$$

The first term $F(q^2)/(q^2)^n$ in each integrand can be obtained simply by expanding the left side of Eq. (B3) in powers of σ . The remaining terms in the integrand subtract the divergent terms in the Laurent expansion of $F(q^2)/(q^2)^n$ in q^2 .

2. Integral over Momentum

The thermal average \mathcal{F}_{cd} is defined in Eq. (B1). If $\Delta_{cd} > m_{\pi cd}$, its real part can be expressed in terms of a principal-value integral that can be reduced to the form in the first term of the second line of Eq. (B3):

$$\text{Re}[\mathcal{F}_{cd}] = \frac{1}{2\pi^2 \mathbf{n}_\pi} \int_0^\infty dq \left(\frac{q^4}{\omega_{cdq}} \mathfrak{f}_\pi(\omega_{cdq}) - \frac{q_{cd}^4}{\Delta_{cd}} \mathfrak{f}_\pi(\Delta_{cd}) \right) \frac{1}{q^2 - q_{cd}^2}, \quad (\text{B5})$$

where $\omega_{cdq} = \sqrt{m_{\pi cd}^2 + q^2}$ and $q_{cd}^2 = \Delta_{cd}^2 - m_{\pi cd}^2$. The denominator has a zero at $q_{cd} = \sqrt{\Delta_{cd}^2 - m_{\pi cd}^2}$. The subtraction of the numerator makes the integral convergent. If $\Delta_{cd} < m_{\pi cd}$, the subtraction at $\omega_{cdq} = \Delta_{cd}$ is not necessary because the integral is convergent.

The imaginary part of \mathcal{F}_{cd} is nonzero only if $\Delta_{cd} > m_{\pi cd}$. It can be evaluated analytically using a delta function as in Eq. (B3):

$$\text{Im}[\mathcal{F}_{cd}] = -\frac{1}{4\pi \mathbf{n}_\pi} \left[\frac{\mathfrak{f}_\pi(\Delta_{cd})}{\Delta_{cd}} q_{cd}^3 \right] \theta(\Delta_{cd} - m_{\pi cd}). \quad (\text{B6})$$

3. Expansion in Isospin Splittings

The thermal average over the Bose-Einstein distribution for a pion is defined in Eq. (21). The thermal average \mathcal{F}_{cd} defined in Eq. (B1) depends on $\Delta_{cd}^2 - m_{\pi cd}^2$, which is linear in isospin splittings. The thermal average can be expanded in powers of $\Delta_{cd}^2 - m_{\pi cd}^2$ using the results presented in Section B 1. The real part can be expanded in integer powers of isospin splittings divided by m_π . The leading term in the expansion of the real part of \mathcal{F}_{cd} is

$$\text{Re}[\mathcal{F}_{cd}] \approx \left\langle \frac{1}{\omega_q} \right\rangle. \quad (\text{B7})$$

The imaginary part of \mathcal{F}_{cd} is nonzero only if $\Delta_{cd} > m_{\pi cd}$. It can be expanded in half-integer powers of isospin splittings divided by m_π . The leading term in the expansion of the imaginary part is

$$\text{Im}[\mathcal{F}_{cd}] \approx \frac{\mathfrak{f}_\pi(m_\pi)}{4\pi \mathbf{n}_\pi} \left(-\frac{1}{m_\pi} q_{cd}^3 \right) \theta(\Delta_{cd} - m_{\pi cd}). \quad (\text{B8})$$

-
- [1] B. Grzadkowski, M. Iglicki and S. Mrówczyński, *t*-channel singularities in cosmology and particle physics, Nucl. Phys. B **984**, 115967 (2022) [arXiv:2108.01757].
[2] R.F. Peierls, Possible Mechanism for the Pion-Nucleon Second Resonance, Phys. Rev. Lett. **6**, 641-643 (1961).

- [3] K. Melnikov and V.G. Serbo, New type of beam size effect and the W boson production at $\mu^+\mu^-$ colliders, *Phys. Rev. Lett.* **76**, 3263 (1996) [arXiv:hep-ph/9601221].
- [4] M. Igllicki, Thermal regularization of t-channel singularities in cosmology and particle physics: the general case, *JHEP* **06**, 006 (2023) [arXiv:2212.00561].
- [5] E. Braaten, R. Bruschini, L.-P. He, K. Ingles and J. Jiang, Evolution of charm-meson ratios in an expanding hadron gas, *Phys. Rev. D* **107**, 076006 (2023) [arXiv:2209.04972].
- [6] S. Weinberg, Phenomenological Lagrangians, *Physica A* **96**, 327-340 (1979).
- [7] G. Burdman and J.F. Donoghue, Union of chiral and heavy quark symmetries, *Phys. Lett. B* **280**, 287 (1992).
- [8] M.B. Wise, Chiral perturbation theory for hadrons containing a heavy quark, *Phys. Rev. D* **45**, R2188 (1992).
- [9] H.Y. Cheng, C.Y. Cheung, G.L. Lin, Y.C. Lin, T.M. Yan and H.L. Yu, Chiral Lagrangians for radiative decays of heavy hadrons, *Phys. Rev. D* **47**, 1030 (1993) [arXiv:hep-ph/9209262].
- [10] S.A. Bass, *et al.*, Microscopic models for ultrarelativistic heavy ion collisions, *Prog. Part. Nucl. Phys.* **41**, 255-369 (1998) [arXiv:nucl-th/9803035].
- [11] P.F. Kolb and U.W. Heinz, Hydrodynamic description of ultrarelativistic heavy ion collisions, [arXiv:nucl-th/0305084].
- [12] F. Gelis, E. Iancu, J. Jalilian-Marian and R. Venugopalan, The Color Glass Condensate, *Ann. Rev. Nucl. Part. Sci.* **60**, 463-489 (2010) [arXiv:1002.0333].
- [13] W. Busza, K. Rajagopal and W. van der Schee, Heavy Ion Collisions: The Big Picture, and the Big Questions, *Ann. Rev. Nucl. Part. Sci.* **68**, 339-376 (2018) [arXiv:1802.04801].
- [14] H. Elfner and B. Müller, The exploration of hot and dense nuclear matter: Introduction to relativistic heavy-ion physics, [arXiv:2210.12056].
- [15] S. Cho *et al.* [ExHIC], Studying Exotic Hadrons in Heavy Ion Collisions, *Phys. Rev. C* **84**, 064910 (2011) [arXiv:1107.1302].
- [16] S. Cho *et al.* [ExHIC], Exotic hadrons from heavy ion collisions, *Prog. Part. Nucl. Phys.* **95**, 279-322 (2017) [arXiv:1702.00486].
- [17] J.D. Bjorken, Highly Relativistic Nucleus-Nucleus Collisions: The Central Rapidity Region, *Phys. Rev. D* **27**, 140-151 (1983)
- [18] C.M. Ko, B. Zhang, X.N. Wang and X.F. Zhang, Charmonium production from hot hadronic matter, *Phys. Lett. B* **444**, 237-244 (1998) [arXiv:nucl-th/9808032].
- [19] L.W. Chen, V. Greco, C.M. Ko, S.H. Lee and W. Liu, Pentaquark baryon production at the Relativistic Heavy Ion Collider, *Phys. Lett. B* **601**, 34-40 (2004) [arXiv:nucl-th/0308006].
- [20] L.W. Chen, C.M. Ko, W. Liu and M. Nielsen, $D_{sJ}(2317)$ meson production at RHIC, *Phys. Rev. C* **76**, 014906 (2007) [arXiv:0705.1697].
- [21] L.M. Abreu, $X_J(2900)$ states in a hot hadronic medium, *Phys. Rev. D* **103**, 036013 (2021) [arXiv:2010.14955].
- [22] P. Braun-Munzinger, K. Redlich and J. Stachel, Particle production in heavy ion collisions, [arXiv:nucl-th/0304013].
- [23] A. Andronic, P. Braun-Munzinger, K. Redlich and J. Stachel, Statistical hadronization of charm in heavy ion collisions at SPS, RHIC and LHC, *Phys. Lett. B* **571**, 36-44 (2003) [arXiv:nucl-th/0303036].
- [24] A. Andronic, P. Braun-Munzinger, M. K. Köhler, A. Mazeliauskas, K. Redlich, J. Stachel and V. Vislavicius, The multiple-charm hierarchy in the statistical hadronization model, *JHEP* **07**, 035 (2021) [arXiv:2104.12754].

- [25] S. Acharya *et al.* [ALICE], Production of charged pions, kaons, and (anti-)protons in Pb-Pb and inelastic pp collisions at $\sqrt{s_{NN}} = 5.02$ TeV, Phys. Rev. C **101**, 044907 (2020) [arXiv:1910.07678].
- [26] A. Andronic, P. Braun-Munzinger, K. Redlich and J. Stachel, Decoding the phase structure of QCD via particle production at high energy, Nature **561**, no.7723, 321-330 (2018) [arXiv:1710.09425].
- [27] J. Gasser and H. Leutwyler, Light Quarks at Low Temperatures, Phys. Lett. B **184**, 83-88 (1987).
- [28] J.L. Goity and H. Leutwyler, On the Mean Free Path of Pions in Hot Matter, Phys. Lett. B **228**, 517-522 (1989).
- [29] A. Schenk, Pion propagation at finite temperature, Phys. Rev. D **47**, 5138-5155 (1993).
- [30] D. Toublan, Pion dynamics at finite temperature, Phys. Rev. D **56**, 5629-5645 (1997) [arXiv:hep-ph/9706273].
- [31] C. Fuchs, B. V. Martemyanov, A. Faessler and M.I. Krivoruchenko, D-mesons and charmonium states in hot pion matter, Phys. Rev. C **73**, 035204 (2006) [arXiv:nucl-th/0410065].
- [32] M. He, R. J. Fries and R. Rapp, Thermal Relaxation of Charm in Hadronic Matter, Phys. Lett. B **701**, 445-450 (2011) [arXiv:1103.6279].
- [33] G. Montaña, À. Ramos, L. Tolos and J.M. Torres-Rincon, Impact of a thermal medium on D mesons and their chiral partners, Phys. Lett. B **806**, 135464 (2020) [arXiv:2001.11877].
- [34] G. Montaña, À. Ramos, L. Tolos and J.M. Torres-Rincon, Pseudoscalar and vector open-charm mesons at finite temperature, Phys. Rev. D **102**, 096020 (2020) [arXiv:2007.12601].
- [35] S. Cho and S.H. Lee, Hadronic effects on the $X(3872)$ meson abundance in heavy ion collisions, Phys. Rev. C **88**, 054901 (2013) [arXiv:1302.6381].
- [36] A. Martinez Torres, K.P. Khemchandani, F.S. Navarra, M. Nielsen and L.M. Abreu, On $X(3872)$ production in high energy heavy ion collisions, Phys. Rev. D **90**, 114023 (2014) [arXiv:1405.7583].
- [37] B. Chen, L. Jiang, X.H. Liu, Y. Liu and J. Zhao, $X(3872)$ Production in Relativistic Heavy-Ion Collisions, Phys. Rev. C **105**, 054901 (2022) [arXiv:2107.00969].
- [38] Y. Hu, J. Liao, E. Wang, Q. Wang, H. Xing and H. Zhang, Production of doubly charmed exotic hadrons in heavy ion collisions, Phys. Rev. D **104**, L111502 (2021) [arXiv:2109.07733].
- [39] L. M. Abreu, F. S. Navarra and H. P. L. Vieira, Multiplicity of the doubly charmed state T_{cc}^+ in heavy-ion collisions, Phys. Rev. D **105**, 116029 (2022) [arXiv:2202.10882].
- [40] H.O. Yoon, D. Park, S. Noh, A. Park, W. Park, S. Cho, J. Hong, Y. Kim, S. Lim and S.H. Lee, $X(3872)$ and T_{cc} : structures and productions in heavy ion collisions, Phys. Rev. C **107**, 014906 (2023) [arXiv:2208.06960].